Transcribed enhancers lead waves of coordinated transcription in transitioning mammalian cells

Arner et al, Science 2015

Auxiliary file 1:Detailed description of time courses

Table of contents:

Adipocyte differentiation

Time course ID: human_mesenchymal_stem_cells_adipose_derived, human_Adipocyte_differentiation

Sample provider: Peter Arner, Niklas Mejhert, Anna Ehrlund, Jurga Laurencikiene, Erik Arner

Introduction

Adipose tissue can account for between 5% (lean athletes) and 60% (morbidly obese) of total body mass, making it one of the most plastic organs in the body [8]. In response to changed nutritional status, both adipocyte cell number and size change and even under stable conditions as much as 10% of the adipocytes are turned over annually [1,2]. Thus the birth of new adipocytes from precursor cells (adipogenesis) is central for a functional fat tissue.

Samples

We are using two different models of human adipogenesis in the FANTOM5 study. Both originate from the stromal-vascular fraction (SVF) of human subcutaneous adipose tissue.
The first model, here called preadipocytes, consists of cells differentiated in vitro directly after SVF isolation from adipose tissue. This means only later stages of differentiation can be monitored as samples in the beginning contain other cell types, like immune and endothelial cells, that contaminates the results. These contaminants die off after approximately 3-4 days. For this model we have taken tissue from four donors and sampled differentiation at time-points 4, 8 and 12 days after differentiation start. We have also isolated mature adipocytes from the adipose tissue of these donors.
For the other model system, here called human adipose-derived mesenchymal stem cells (hASC), we have propagated cells from the SVF in vitro thus selecting for a stem cell/progenitor population. These cells can be expanded and cultured for several passages. This gives us cells with a homogenous genetic background and since contaminants are removed from the beginning, differentiation can be monitored from start to finish. Here we have collected triplicate samples at 0, 15, 30, 45 min, 1 h, 1 h 20 min, 1 h 40 min, 2 h, 2 h 30 min, 3 h, 12 h and 1, 2, 4, 8, 12 and 14 days after differentiation start.

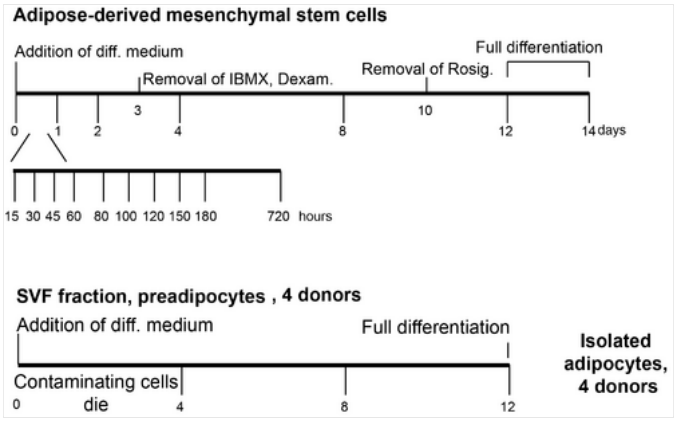

Figure 1. Sample collection scheme for the different model system. Sample collection time points are indicated as well as the removal of some components of the differentiation cocktail. IBMX=3-isobutyl-1-methylxanthine, Dexam.=dexamethasone, Rosig.=Rosiglitazone.

Growth conditions

SVF preadipocytes to adipocytes:

Cells were isolated from human adipose tissue as decribed in [3,4,5].

Culture medium used:
Day 1-6: DMEM (1mg/ml glucose), PEST, Fungizone, 15 mM HEPES, 100 nM Cortisol, 66 nM Insulin, 10 µg/ml Transferrin, 33 µM Biotin, 17 µM Panthothenate, 1 nM T3, 10 µM Rosiglitazone
Day 6-12: Same as above but without Rosiglitazone

hASC (human Adipose-derived mesenchymal stem cells):

Cells were isolated, expanded and differentiatied as described in [5,6,7].

Culture medium used:

Proliferation medium: DMEM (1 mg/ml glucose), PEST, 10% FBS, 15 mM HEPES, 2 mM Glutamine, 2.5 ng/ml FGF2
Differentiation start, day 0-3: DMEM/F12 (1:1), PEST, 5 µg/ml Insulin, 10 µg/ml Transferrin, 0.2 nM T3, 100 µM IBMX, 1 µM Dexamethasone, 1 µM Rosiglitazone
Differentiation day 3-9: DMEM/F12 (1:1), PEST, 5 µg/ml Insulin, 10 µg/ml Transferrin, 0.2 nM T3, 1 µM Rosiglitazone
Differentiation day 9-14: DMEM/F12 (1:1), PEST, 5 µg/ml Insulin, 10 µg/ml Transferrin, 0.2 nM T3

Quality control

A key aspect of adipocyte maturation is the accumulation of lipid in intracellular lipid droplets. The accumulation of lipids can be seen as morphological changes in the microscope at low magnification (10x) and can be further visualized using lipid stains such as bodipy (shown below for day 8 and 12).

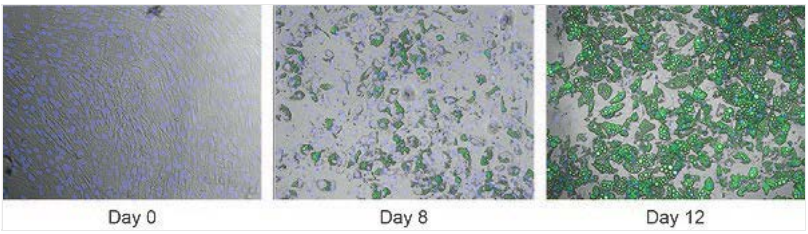

Figure 2: Lipid accumulation during differentiation. hASC cells were stained with Hoechst (nuclei, blue) day 0, 8 and 12 and Bodipy (neutral lipids, green) at day 8 and 12 during differentiation. An overlay of phase contrast and fluorescent image is shown.

Marker gene expression:

Preadipocyte, CAGE:

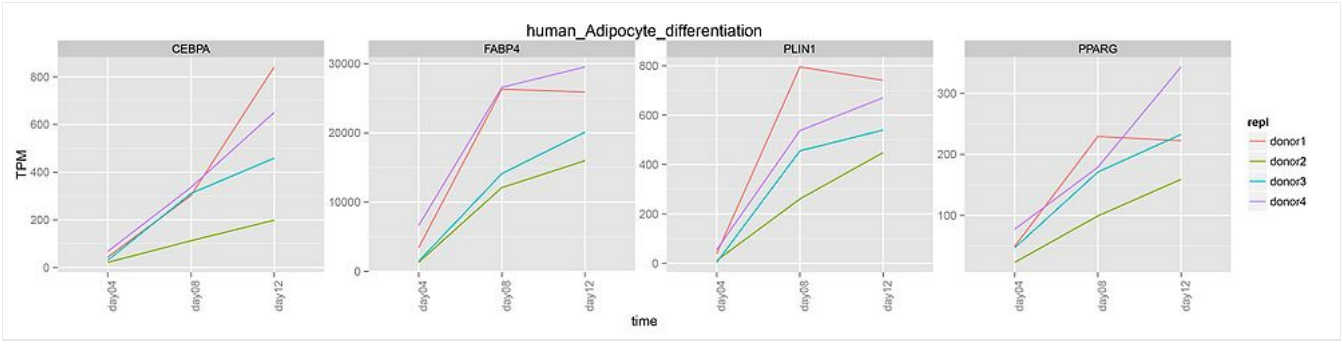

hASC, CAGE:

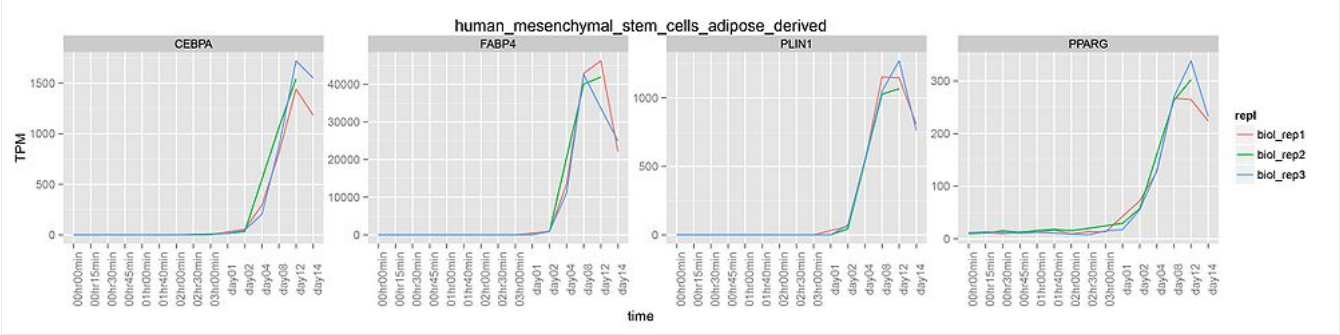

hASC, qPCR

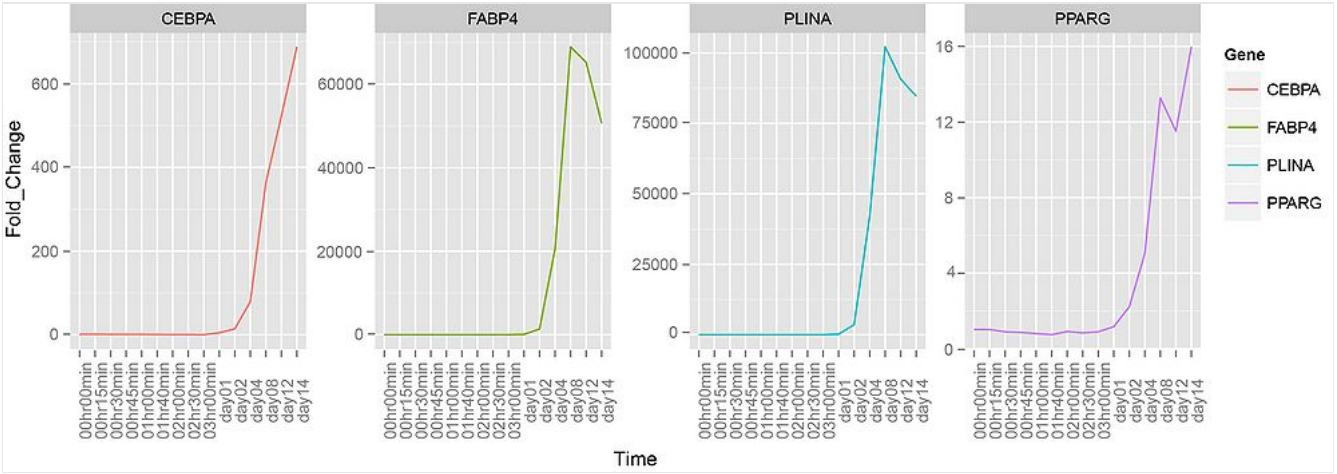

References

[1] Dynamics of fat cell turnover in humans. Spalding KL et al, Nature, 2008, vol 453, p783-787. PMID:18454136

[2] Adipocyte turnover:relevance to human adiopose tissue morphology- Arner E et al, Diabetes, 2010,59(1):105-9. PMID:19846802

Primary preadipocyte isolation and differentiation

[3] van Harmelen V, Skurk T, Hauner H (2005) Primary culture and differentiation of human adipocyte precursor cells. Methods Mol Med 107:125–135

[4] Dicker A, Le Blanc K, Astrom G et al (2005) Functional studies of mesenchymal stem cells derived from adult human adipose tissue. Exp Cell Res 308:283–290

[5] Pettersson AM, Stenson BM, Lorente-Cebrián S, Andersson DP, Mejhert N, Krätzel J, Aström G, Dahlman I, Chibalin AV, Arner P, Laurencikiene J. LXR is a negative regulator of glucose uptake in human adipocytes. Diabetologia. 2013 Sep;56(9):2044-54.

Isolation, propagation and differentiation of hASCs

[5] Pettersson AM, Stenson BM, Lorente-Cebrián S, Andersson DP, Mejhert N, Krätzel J, Aström G, Dahlman I, Chibalin AV, Arner P, Laurencikiene J. LXR is a negative regulator of glucose uptake in human adipocytes. Diabetologia. 2013 Sep;56(9):2044-54.

[6] Rodriguez AM , Pisani D , Dechesne CA , et al.. Transplantation of a multipotent cell population from human adipose tissue induces dystrophin expression in the immunocompetent mdx mouse. J Exp Med. 2005;201:1397–1405.

[7] Zaragosi LE , Ailhaud G , Dani C. Autocrine fibroblast growth factor 2 signaling is critical for self-renewal of human multipotent adipose-derived stem cells. Stem Cells. 2006;24:2412–2419.

References on adipocyte differentiation in general

[8] Cawthorn WP, Scheller EL, MacDougald OA., Adipose tissue stem cells meet preadipocyte commitment: going back to the future. J Lipid Res. 2012 Feb;53(2):227-46.

[9] Forming functional fat: a growing understanding of adipocyte differentiation. Cristancho AG, Lazar MA. Nat Rev Mol Cell Biol. 2011 Sep 28;12(11):722-34. PMID:21952300

[10] Propagation of adipogenic signals through an epigenomic transition state. Steger DJ, Grant GR, Schupp M, Tomaru T, Lefterova MI, Schug J, Manduchi E, Stoeckert CJ Jr, Lazar MA. Genes Dev. 2010 May 15;24(10):1035-44. PMID:20478996

Primary Aortic Smooth Muscle Cells (AoSMC) Response to Interleukin-1beta (IL1-beta) and Fibroblast Growth Factor-2 (FGF-2)

Time course ID: human_Aortic_smooth_muscle_cell_FGF2 and human_Aortic_smooth_muscle_cell_IL1b
Sample provider: Levon Khachigian, Margaret Patrikakis, Ahmad M.N. Alhendi

Introduction

Vascular smooth muscle cells (SMCs) are key components in our blood vessels, and show remarkable plasticity. SMCs are normally growth-quiescent in the normal adult vessels, but are activated by injury, or exposure to growth factors, such as fibroblast growth factor-2 (FGF-2) and pro-inflammatory cytokines, such as interleukin-1beta (IL-1beta). These cues are sensed by these cells through changes in immediate-early gene expression, and can lead to increased proliferation and migration. These responses are associated with the initiation and progression of a range of vascular diseases including atherosclerosis, post-angioplasty restenosis and bypass graft stenosis.

Samples

We provided total RNA (in triplicate) from growth arrested human aortic SMCs (Cell Applications) treated with IL-1beta or FGF-2 for periods of up to 6 hours. SMCs (pool of 3 donors) were grown in 100 mm petri dishes in Waymouth's medium, pH 7.4, supplemented with 1 mM L-glutamine, 10 units/ml penicillin, 10 mcg/ml streptomycin and 10% fetal bovine serum, at 37°C in a humidified atmosphere of 5% CO2. The cells were rendered growth-quiescent at 80-90% confluency by incubation in serum-free medium for 24h. The SMCs were then exposed to IL-1beta (10ng/ml) or FGF-2 (50ng/ml) for various times up to 6 hours (0, 15, 30, 45, 60, 120, 180, 240, 300 and 360 min). 0 min samples represent growth arrested and unstimulated cells. RNA was harvested using TRIzol reagent, quantitated using a Nanodrop spectrophometer and validated for the transient induction of Egr-1 mRNA (by quantitative real-time PCR) prior to shipment to the Omics Science Center, RIKEN Yokohama Institute (Japan) for CAGE analysis.

Quality control

Early growth response-1 (Egr-1) is an immediate-early gene (encoding a zinc finger transcription factor) that is poorly expressed in growth-quiescent cells and serves as a marker of cell activation or stress. Total RNA provided to the RIKEN Yokohama Institute was first analysed for Egr-1 expression by qRT-PCR. This demonstrated peak inducible expression after 30 min by FGF-2 and after 60 min by IL-1beta (Fig 1). Transient expression of this biomarker within 30-60 min is supported by the literature (e.g. Zhu et al. 2007).

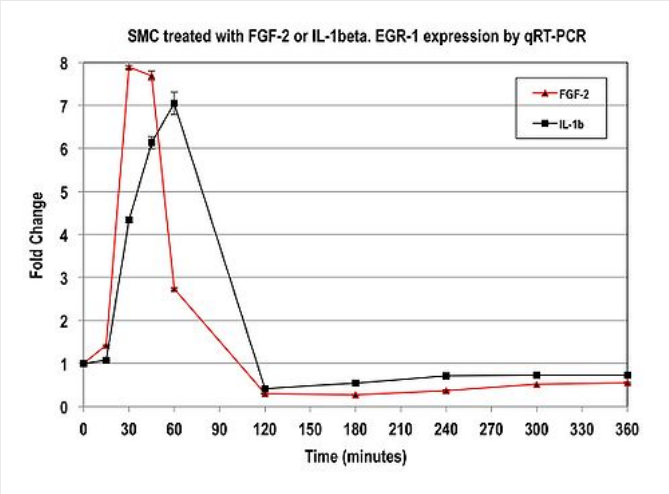

Figure 1 (qRT-PCR analysis, EGR-1)

CAGE analysis on these samples revealed that Egr-1 underwent transient induction within 30-60 min in response to the growth factor or cytokine (Fig 2). In contrast, CAGE analysis revealed no change in expression of alpha-actin 2 (ACTA2) in response to FGF-2 or IL-1beta within the 6h time frame (Fig 2).

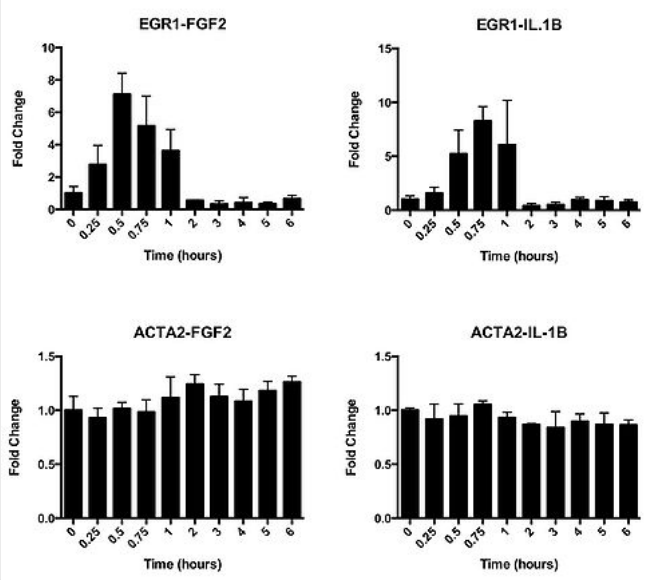

Figure 2 (CAGE analysis, EGR-1 and ACTA2)

CAGE analysis (Fig 3) and subsequent qRT-PCR analysis using separate samples in which Egr-1 was induced (Fig 4) also revealed dynamic changes in the expression of two other prototypic immediate-early genes, c-FOS and FOSB, in response to FGF-2 or IL-1beta (Fig 5).

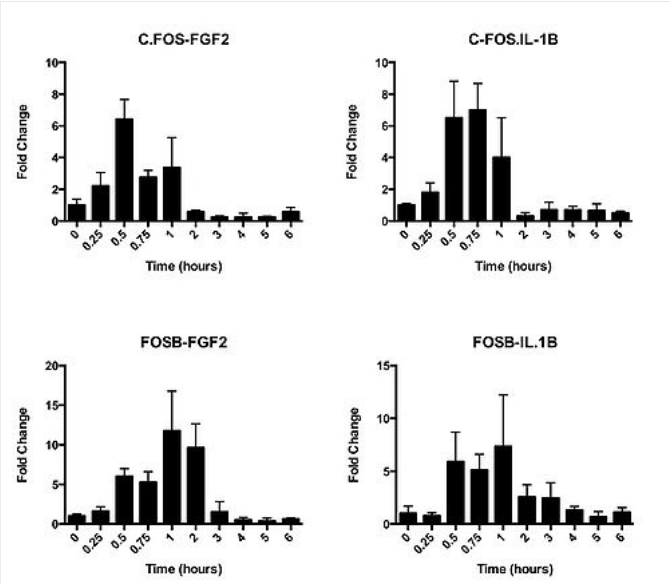

Figure 3 (CAGE analysis, c-FOS and FOSB)

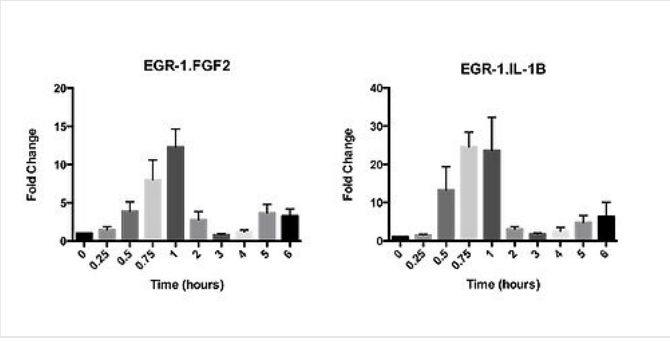

Figure 4 (qRT-PCR analysis, EGR-1)

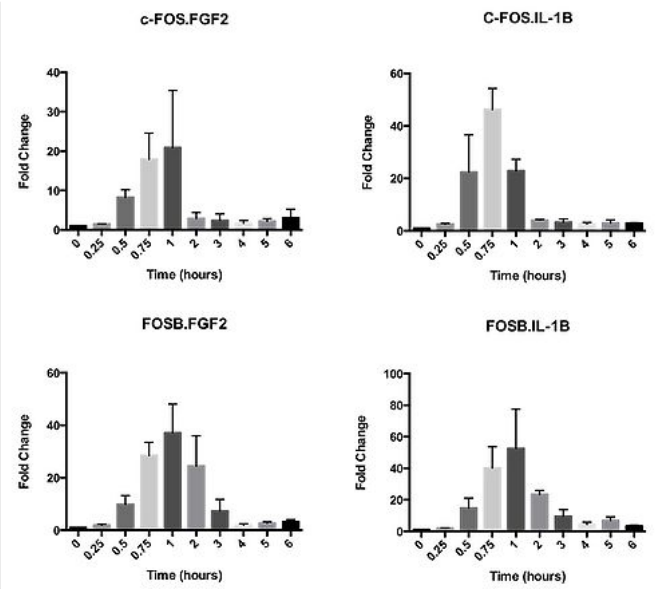

Figure 5 (qRT-PCR analysis, c-FOS and FOSB)

References

[1] Zhu et al. Cardiovasc Res. 2007;76(1):141-8 [2] Silverman et al. Am J Pathol. 1999;155(4):1311-7

Retinal pigment mesenchyme transition

Time course ID: human_ARPE-19
Sample provider: Soichi Ogishima, Hiroshi Tanaka, Ken Miyaguchi, Afsaneh Eslami

Introduction

Epithelial–mesenchymal transition (EMT) is a process of transition from epithelial cells to mesenchymal cells characterized by loss of cell adhesion and polarity, repression of E-cadherin expression, gain of cell motility and nvasive properties. EMT is essential for numerous developmental processes including mesoderm formation and neural tube formation. EMT is also essential for wound healing, organ fibrosis and initiation of metastasis for cancer progression. During the process of epithelial to mesenchymal transition, epithelial cells transforms to mesenchymal cells, and change their shapes. Mesenchymal cells get to gather and form focus. To clarify the transcriptional networks regulating EMT, we obtained time-course sample of human ARPE-19 epithelial to mesenchymal transition. After preculture for 7 days on 10cm dishes and cell seeding and cell culture for 5 days on 6-well glass bottom plate, we induced epithelial to mesenchymal transition on human ARPE-19 cells by TT-mixture of TNFα and TGFβ2. Triplication for RNA extraction and 1 for imaging. We sampled total RNA of human ARPE-19 cells along with time-course of epithelial to mesenchymal transition.

Samples

ARPE-19 cells were cultured in Dulbecco's Modified Eagle's Medium/Nutrient Mixture F-12 medium (Sigma-Aldrich) with 10% fetal bovine serum in a CO2 incubator at 37 °C. After 5 days of preculture, cells were treated with human recombinant TGF-β2 and human recombinant TNF-α and continuously incubated in serum free medium at 37 °C to induce EMT. At 21 different time points (0 min, 15 min, 30 min, 45 min, 60 min, 80 min, 100 min, 2 hr, 2.5 hr, 3 hr, 3.5 hr, 4 hr, 5 hr, 6 hr, 7 hr, 8 hr, 12 hr, 16 hr, 24 hr, 42 hr and 60 hr), cells were dissolved in lysis reagent and collected. For the samples of 0 min, cells were treated with PBS without TGF-β2 and TNF-α. Using miRNeasy Mini Kit (QIAGEN), total RNA was extracted from each cell lysate according to a manufacturer's protocol.

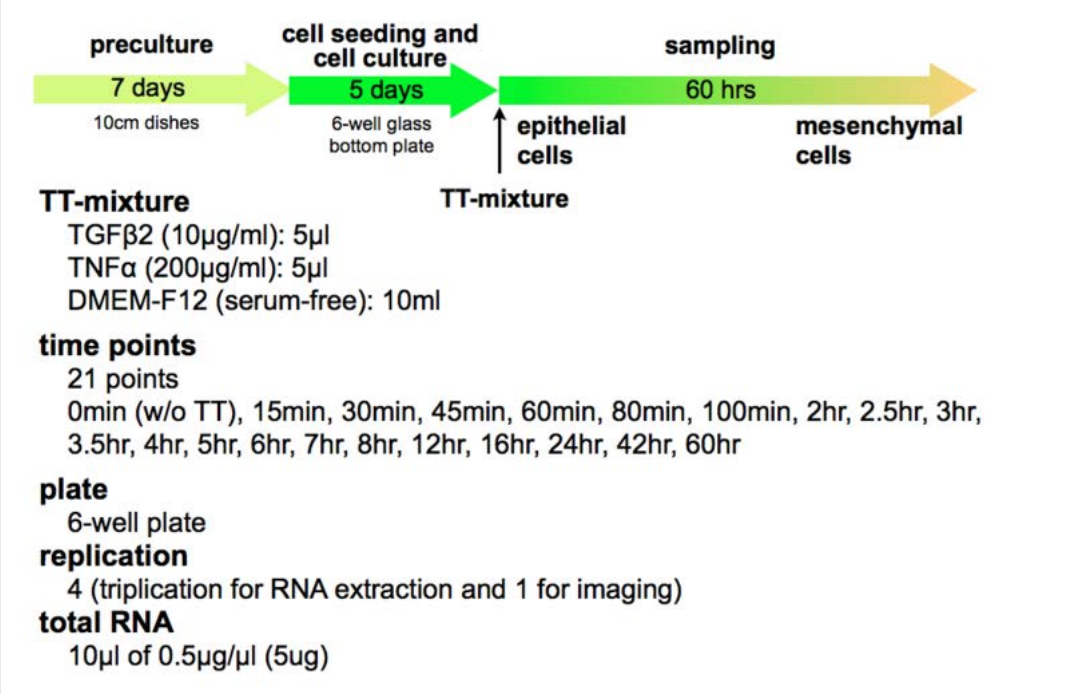

Figure 1: Sample protocol

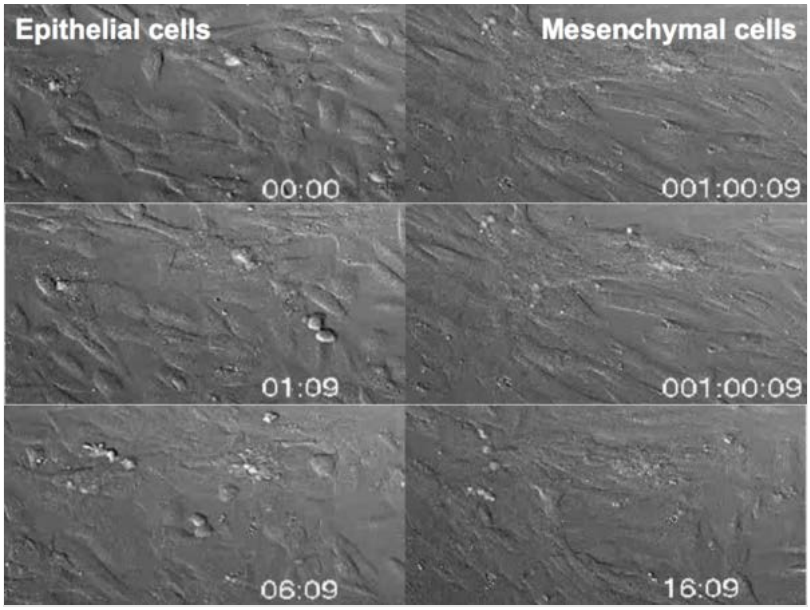

Figure 2: Cell morphology

Quality control

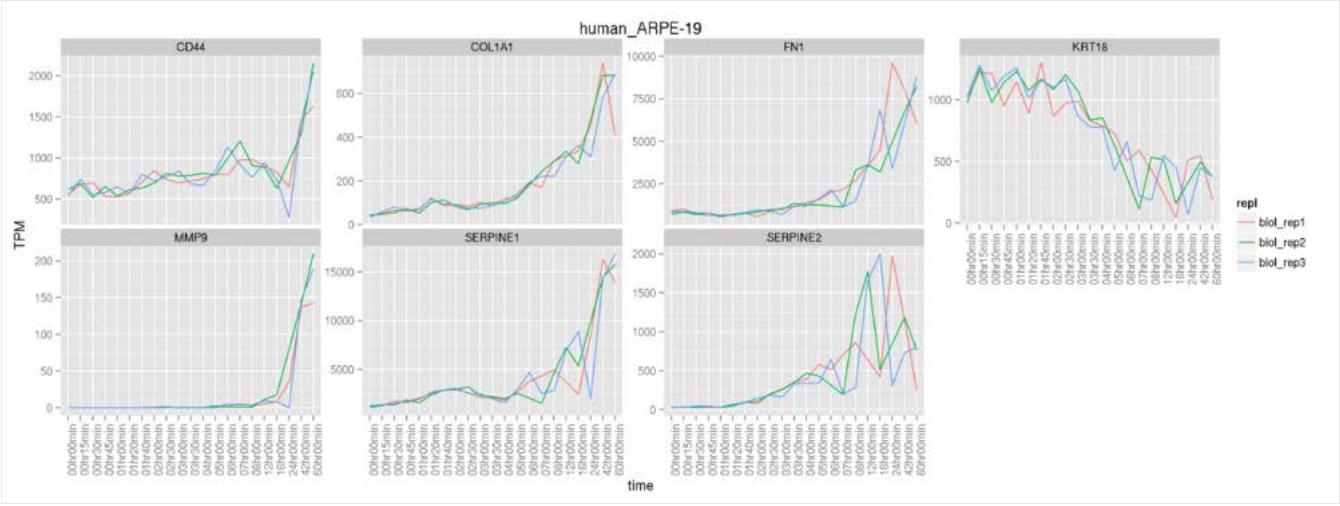

Figure 3: CAGE expression of marker genes in TPM.

References

[1] Tumor necrosis factor-alpha regulates transforming growth factor-beta-dependent epithelial-mesenchymal transition by promoting hyaluronan-CD44-moesin interaction. Takahachi E et al, J Biol Chem, 2010, 285(6):4060-73. PMID:19965872

[2] Epithelial-mesenchymal transitions in development and disease, Thiery JP et al, Cell, 2009, 139(5):871–890. PMID:19945376

Melanocytic differentiation

Time course ID: human_H9

Meenhard Herlyn, Rolf Swoboda

Introduction

Melanocytes are pigment producing cells that reside in and supply melanin to the skin and eyes. These specialized cells are developmental derived from the neural crest and undergo programmed differentiation throughout migration and terminal differentiation upon reaching their final residential destination. While most melanocyte development studies have been assessed in avian and murine models, capturing their differentiation regulatory networks has been difficult due their vast and speedy migration throughout the embryo. Very few studies have documented human melanocyte development. In an effort to reconcile these discrepancies we have developed a method to efficiently differentiate human embryonic stem cells to terminally differentiated pigmented melanocytes (1, 2) Utilizing this differentiation approach we hope to gain insight into pathways active during human melanocyte differentiation.

Samples

For the FANTOM5 study the human embryonic stem cell line H9 [WA09 (MEF platform), WiCell Research Institute] was used to study human melanocyte development. In this model, human embryoid bodies (H9EB) were first generated from undifferentiated H9ES for 4 days in suspension culture conditions. H9EBs were then harvested and differentiated on fibronectin-coated flasks in melanocyte differentiation media (Mel-1). The exact protocol has been published by Zabierowski and Herlyn (2). Briefly 70 – 80% confluent feeder-based ES colonies grown in 6-well plates were gently scraped with a cell lifter into T25 flasks (one 6 well plate per T25) and incubated overnight with EB medium at 37oC. The next day cells were transferred into new T25 flasks with fresh EB medium taking care not to disrupt cell clusters. 2/3 of the EB medium was replenished every day for the next 3 days. On day 4 (day 0 of time course) embryoid bodies were harvested and carefully transferred onto 10 ng/ml fibronectin coated T25 flasks with Mel-1 differentiation medium. 2/3 of the differentiation medium was replenished every other day. On day 24 cells were dissociated into single-cells with trypsin/EDTA treatment and replated onto fresh fibronectin-coated T25 flasks (1:1 passage) in Mel-1 without TPA. 2/3 Mel-1 medium without TPA was replenished every 2-3 days. RNA samples were harvested from T25 flasks by direct lysis on days 1, 3, 6, 9, 12, 15, 18, 21, 24, 27, 30, 33, 36, 39 and 42 following the QIAGEN RNeasy Kit protocol. RNA yielded from all samples was stored at -80 C. This time course was repeated in triplicate. For each replicate, H9EB (day 0, embryoid bodies prior to plating in melanocyte differentiation media) and undifferentiated H9ES cells were included as negative controls. Additionally, 3 different human foreskin derived melanocyte cell lines were included as positive controls.

Media: a) Embryoid body (EB) medium (100 ml): 80 ml DMEM/F-12 (Invitrogen #11330-032), 20 ml Knockout-Serum Replacer (Invitrogen #10828-028), 1 ml 200 mM L-glutamine (Invitrogen #21051-024), + 0.7 ml b-mercaptoethanol/1 ml L-glutamine, 1 ml nonessential amino acids 100X (Invitrogen #11140).

b) Mel-1 medium for melanocyte differentiation (100 ml): 20 ml Dexamethasone (Sigma #D-2915 – make up to 0.25 M in water and store at –20 C), 1 ml ITS Liquid Medium Supplement (Sigma #I-3146), 1 ml Linoleic Acid-BSA (Sigma #L-9530), 30 ml DMEM-Low Glucose (Invitrogen #11885),20 ml MCDB201, 1 ml L-ascorbic acid (Sigma #A-4403), 50 ml Wnt3a conditioned medium), 1 ml Stem Cell Factor (Fitzgerald Industries #RDI-118B-218 – make up to 10 mg/ml in 0.1% BSA in 1X DPBS and store stock at –70 C), 100 ml Basic Fibroblast Growth Factor (Fitzgerald Industries #RDI-118B-218 – make up to 4 mg/ ml in 0.1% BSA in 1X DPBS and store stock at –70oC), 100 ml Endothelin-3 (American Peptide Co. #88-5-10 – make up264 mg/ml in 0.1% BSA in 1X DPBS and store stock at –70 C), 150 ml Cholera toxin (Sigma #C-3012 – make up to 3.32 mg/ml in 0.1% BSA in 1X DPBS and store stock at 4 C), 12.5 ml TPA (Sigma #P-1583 – make up to 250 mg/ml in 0.1% BSA in 1X DPBS and store stock at –20 C).

c) L-Wnt3A conditioning medium: 1% FBS (1000 ml): 900 ml DMEM (Cellgro #10-017-CM), 10 ml FBS.

d) L-Wnt3A conditioned medium: Confluent L-Wnt3A cells were split 1:10 into L-Wnt3A conditioning medium. The cells were grown 4 days at 37 C. The supernatant was harvested , filter sterilized and stored as batch 1.Fresh conditioning medium was added to the cells and cultured for another 3 days. The medium was harvested, filter sterilized and mixed 1:1 with batch 1.

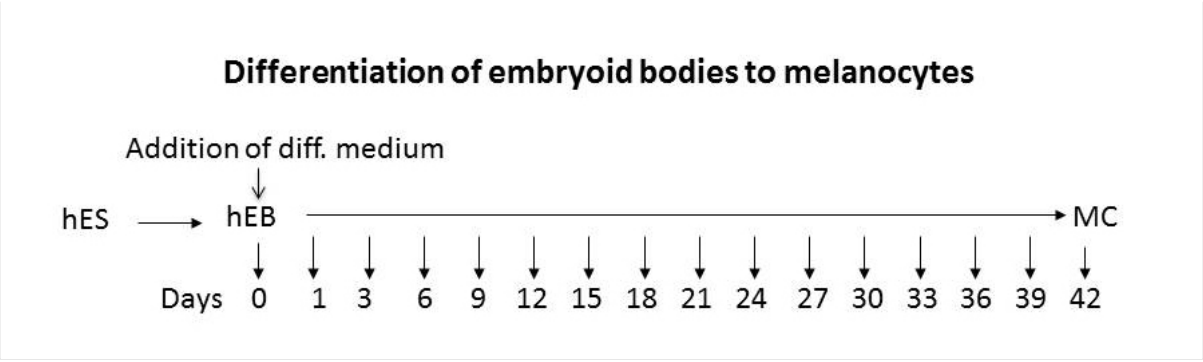

Quality control

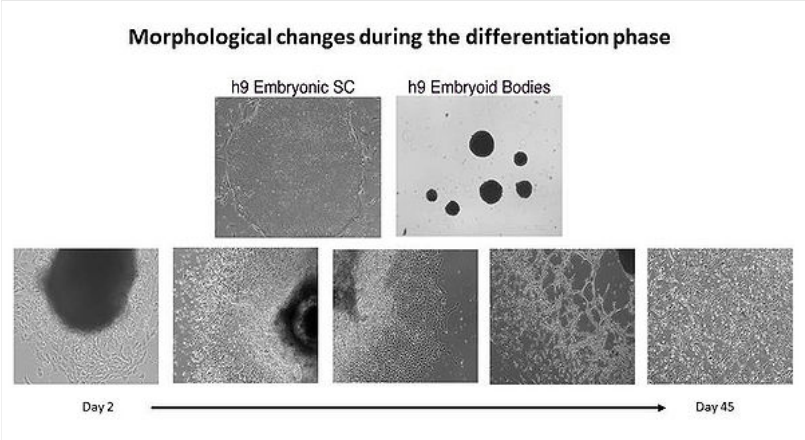

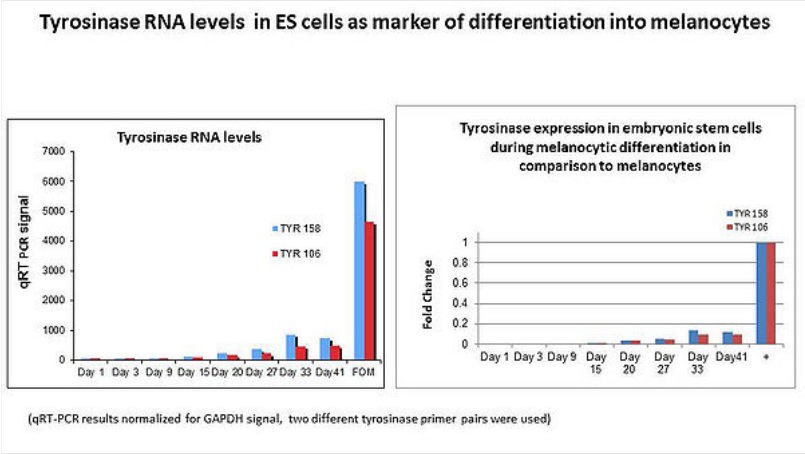

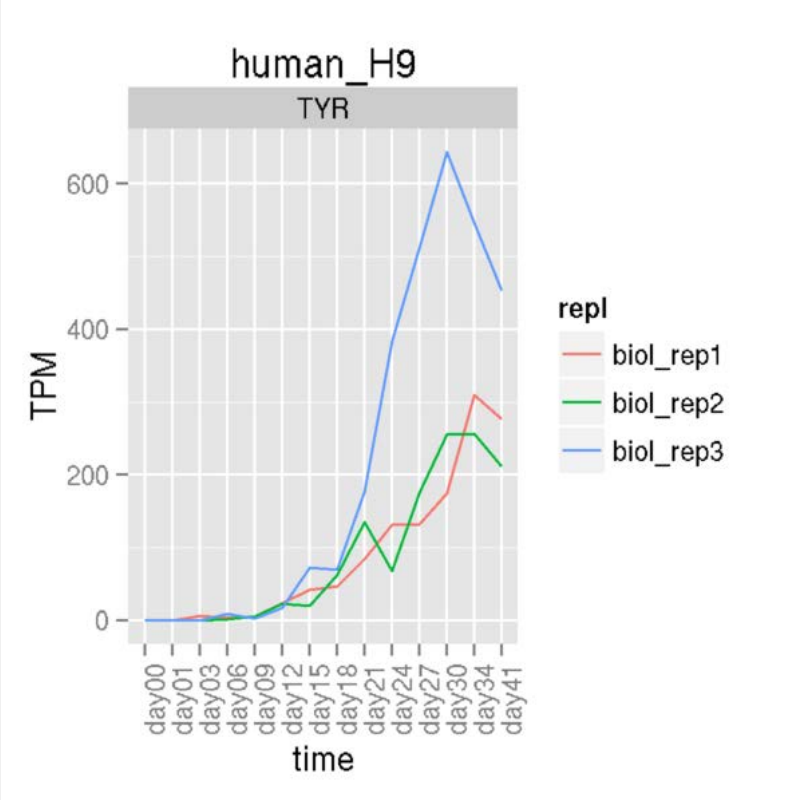

Figure 2: CAGE expression of marker genes in TPM.

References

1. Defining the conditions for the generation of melanocytes from human embryonic stem cells.

[1] Fang D, Leishear K, Nguyen TK, Finko R, Cai K, Fukunaga M, Li L, Brafford PA, Kulp AN, Xu X, Smalley KS, Herlyn M. Stem Cells. 2006 Jul;24(7):1668-77.

2. Embryonic stem cells as a model for studying melanocyte development.

[2] Zabierowski SE, Herlyn M. Methods Mol Biol. 2010;584:301-16.

Cardiomyocyte differentiation

Time course ID: human_HES3-GFP_Embryonic_Stem_cells
Sample provider: Christine Mummery and Robert Passier

Introduction

Human H3 embryonic stem cells differentiated to cardiomyocytes

Human pluripotent stem cells have the potential to differentiate to all cell types of the human body, including cardiomyocytes. Since the adult human heart does not have the capacity to regenerate, loss of cardiomyocytes after myocardial infarction eventually may lead to heart failure[1]. Cardiomyocytes derived from human pluripotent stem cells may represent a source for future cell replacement in patients with cardiac injury. Furthermore, human cardiomyocytes may also be used for toxicity screening, drug discovery, and for studying mechanisms related to cardiac disease and development. It is important to study the regulatory molecular networks during cardiomyocyte differentiation in order to get a better understanding of processes such as specification, maturation and proliferation of cardiomyocytes. This will lead most likely to novel insights regarding endogenous cardiac regeneration, tissue engineering and cardiac disease.

Samples

For the differentiation of human pluripotent stem cells we used the human embryonic stem cell line HES3-GFP, ubiquitously expressing GFP. Previously, we have shown that co-culture of human embryonic stem cells with a mouse endoderm cell line, END-2, lead to beating cardiomyocytes within 12 days. END-2 cells were treated with mitocmycin C to block proliferation. In general, using this differentiation procedure (in the absence of serum) beating clusters contained 25 % cardiomyocytes[2], [3]. END-2 cells are cultured as a monolayer, whereas differentiated stem cells are grown on top as three-dimensional structures, which allows separation of human embryonic stem cell-derived populations. From undifferentiated human embryonic stem cells and every day during cardiomyocyte differentiation until day 12 samples were collected and used for RNA isolation (n=3).

Quality control

Expression of key markers for this differentiation course is based on previous experiments[4]. For undifferentiated stem cells, OCT4, NANOG, SOX2 are expressed at high levels. At day 3 we expect higher expression levels of MESP1, WNT3A, BrachyuryT. At day MEF2C, TBX5, NKX2.5 should be expressed at higher levels. Finally, at day 12, ACTN2, TNNT, PLN are expressed at high levels.

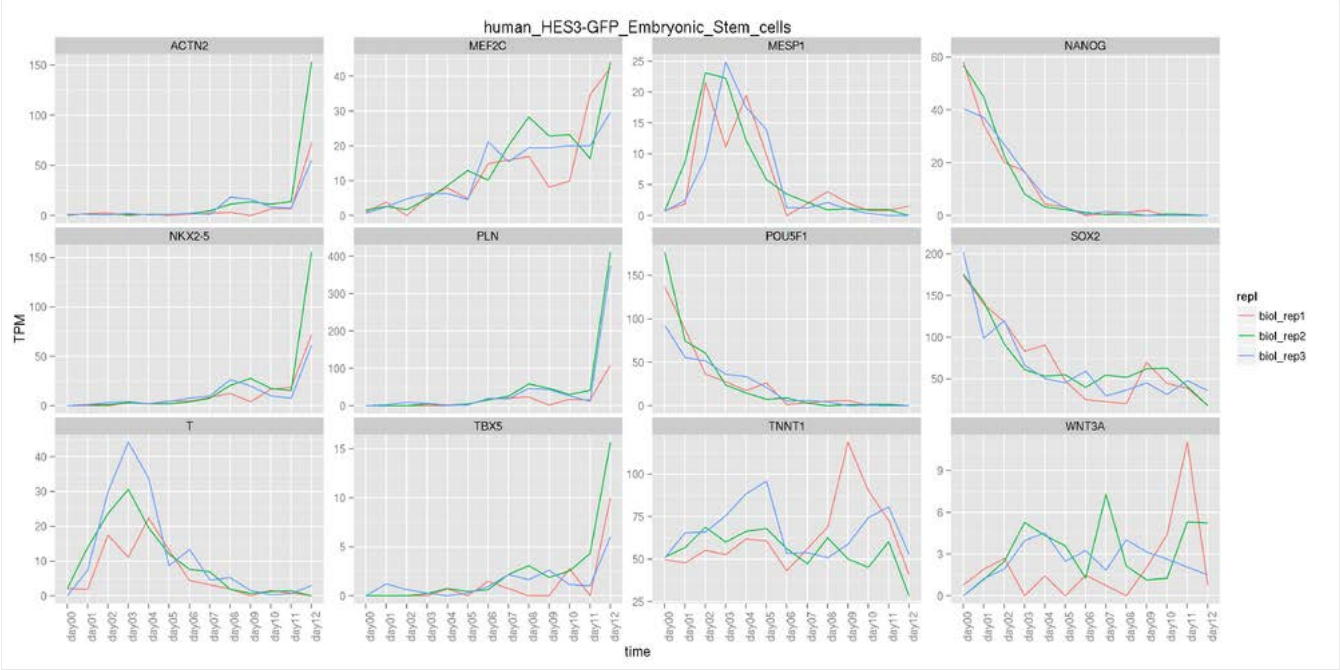

Figure 1: CAGE expression of marker genes in TPM.

References

[1] C. L. Mummery, J. Zhang, E. S. Ng, D. A. Elliott, A. G. Elefanty, and T. J. Kamp, “Differentiation of human embryonic stem cells and induced pluripotent stem cells to cardiomyocytes: a methods overview.,” Circ. Res., vol. 111, no. 3, pp. 344–358, Jul. 2012.

[2] R. Passier, D. W.-V. Oostwaard, J. Snapper, J. Kloots, R. J. Hassink, E. Kuijk, B. Roelen, A. B. de la Riviere, and C. Mummery,

“Increased cardiomyocyte differentiation from human embryonic stem cells in serum-free cultures.,” Stem Cells, vol. 23, no. 6, pp. 772–780, Jun. 2005.

[3] C. Mummery, D. Ward-van Oostwaard, P. Doevendans, R. Spijker, S. van den Brink, R. Hassink, M. van der Heyden, T. Opthof, M. Pera, A. B. de la Riviere, R. Passier, and L. Tertoolen, “Differentiation of human embryonic stem cells to cardiomyocytes: role of coculture with visceral endoderm-like cells.,” Circulation, vol. 107, no. 21, pp. 2733–2740, Jun. 2003.

[4] A. Beqqali, J. Kloots, D. Ward-van Oostwaard, C. Mummery, and R. Passier, “Genome-wide transcriptional profiling of human embryonic stem cells differentiating to cardiomyocytes.,” Stem Cells, vol. 24, no. 8, pp. 1956–1967, Aug. 2006.

Neuronal timecourse

Time course ID: human_iPS_differentiation_to_neuron_down-syndrome-C11, human_iPS_differentiation_to_neuron_down-syndrome-C18, human_iPS_differentiation_to_neuron_control-C11, human_iPS_differentiation_to_neuron_control-C32

Sample provider: Christine Wells, Ernst Wolvetang, James Briggs, Dmitry Ovchinnikov

Introduction

Human induced pluripotent stem cells can generate every cell type of the human body and under the appropriate conditions recapitulate central aspects of embryonic development in the dish. To interrogate the transcriptome changes associated with the earliest steps of human brain development as recapitulated with human pluripotent stem cells we generated footprint-free induced pluripotent stem cells (iPSC) from control and Down syndrome fibroblasts using episomal reprogramming [1] and were next stepwise differentiated these iPSc into neuro-ectodermal cells (day6), neural stem cells (day12) and early neuronal progenitors (day 18) using an established neuronal differentiation protocol [2].

Samples

For this study three sample donors were used, two 2 control iPSC (C11 iPSC derived from CRL2429 Newborn Male Caucasian fibroblasts and C32 iPSC derived from CRL1502 12wk gestation Female Black fibroblasts) and two iPSC clones from one Down Syndrome individual (C11 and C18 from an Unknown Male Caucasian). Three replicates of each iPSc line were subjected to neuronal differentiation as described [1,2] and harvested at day 0, 6, 12, 18 of differentiation for RNA extraction (Fig 1 below).

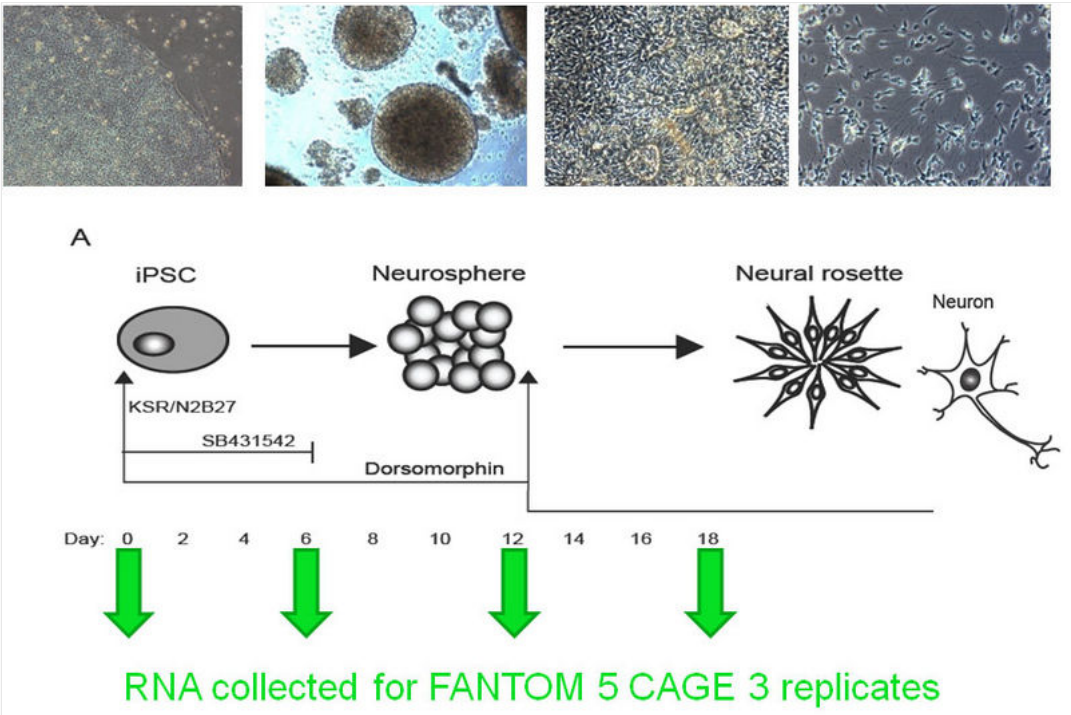

Figure 1: Phase microscope images of neuronally differentiated hIPSC (C32 shown) and a graphical depiction of the timepoints where RNA was harvested for CAGE analysis.

Quality control

Q-PCR validation of key neuronal marker genes was performed and published [1]. The data show upregulation of mRNA expression of the neuronal marker genes PAX6 [3] , beta-III-tubulin [4], SOX1 [5] , DCX [6], SOX9 [7], SOX2 [8] and MASH1 [9] (Fig 2C and D) and robust expression of PAX6, beta-III-Tubulin and MAP2 [10] protein expression (Fig 2A). we further expect that as cells exit from pluripotency that they will display a downregulation of the pluripotency transcription factor Oct4 [11] and the DNA methyl transferase DNMT3B [12].

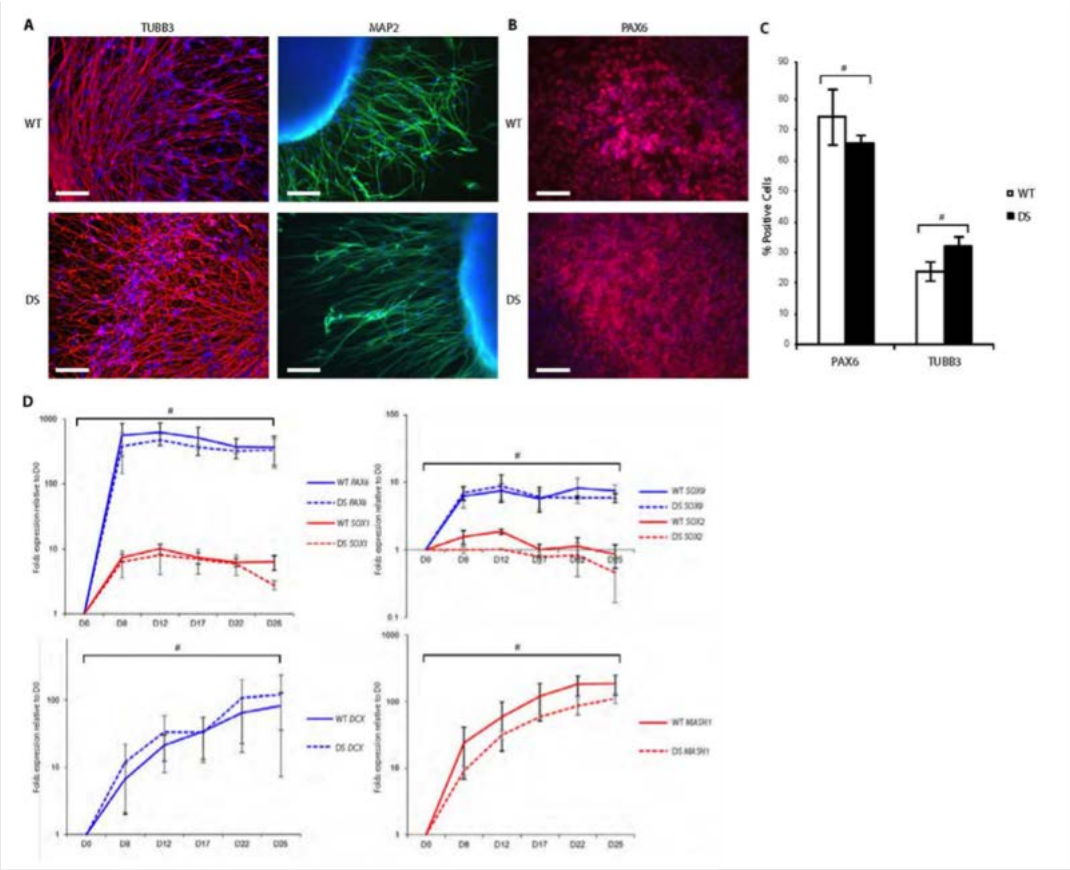

Figure 2: Immunofluorescent detection of neuronal marker proteins beta-III-tubulin, MAP2 and PAX6 in neuronally differentiated hIPSc cultures (A) and Q-PCR mRNA expression quantification of key neuronal genes (B and C) in these samples. Reproduced from [1].

Sample culture information:

hIPS cell culture

Human iPS cells were cultured under feeder-free culture conditions on Matrigel (1:50 dilution BD Biosciences) with mouse embryonic fibroblast conditioned DMEM/F12 culture medium supplemented with 20% KnockOut serum replacement (KOSR), 0.1 mM non-essential amino acids, 1 mM L-glutamine, 0.1 mM ß-mercaptoethanol in the presence of 100 ng/ml human bFGF. Medium was exchanged daily. These cells were next FACS sorted for the cell surface marker TRA160, to ensure isolation of RNA from 100% undifferentiated cells at timepoint 0.

Neural differentiation of hIPS cells

hiPSC cultures were grown for ~5 days after mechanical passage in conditioned medium (as above), and changed directly into KOSR supplemented with 10 μM SB431542 (Sigma) and 5 μM dorsomorphin (Stemgent) for the first 6 and 12 days of differentiation, respectively, with media changes every 2 days to initiate neural conversion. KOSR was gradually substituted with N2B27 medium (Neurobasal medium supplemented with Glutamax, N2 and B27 supplements (all from Gibco)): 25%, 50%, 75% and 100% N2B27 in KOSR on days 4, 6, 8 and 10 respectively. Neurospheres were formed on day 6 of differentiation by 10 min incubation in 1 mg/ml Collagenase IV (Gibco) at 37°C and dislodging of large pieces of colonies by use of a cell scraper and P1000 pipette. Neuralized colony fragments were seeded into Ultra-low Cluster plates (Costar) where they aggregated into tight spheres. Neurospheres were expanded in Ultra-low Cluster plates until day 12 and seeded onto Matrigel (BD), and N2B27 media was changed every 3 days. Adherent cultures were passaged every 4-5 days by cell dissociation buffer (Sigma) at a 1:2 – 1:3 ratio until day 18.

CAGE data

Figure 3 A-D shows the CAGE expression of DNMT3B, MAP2, PAX6, beta-III-tubulin and Oct4 in the two two DS iPSC (A and B) and control iPSC (C and D) subjected to neuronal differentiation. The expected down regulation of the pluripotency markers and upregulation of neuronal identity genes is observed.

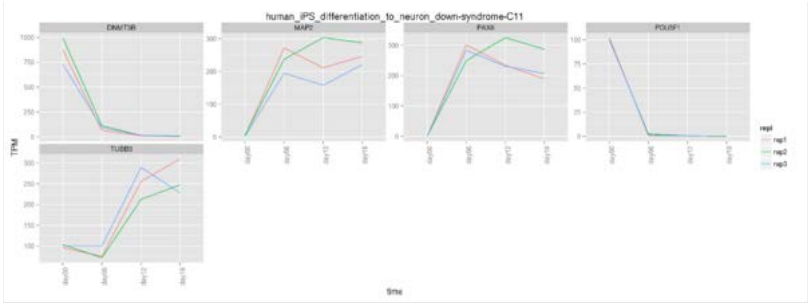

Figure 3A

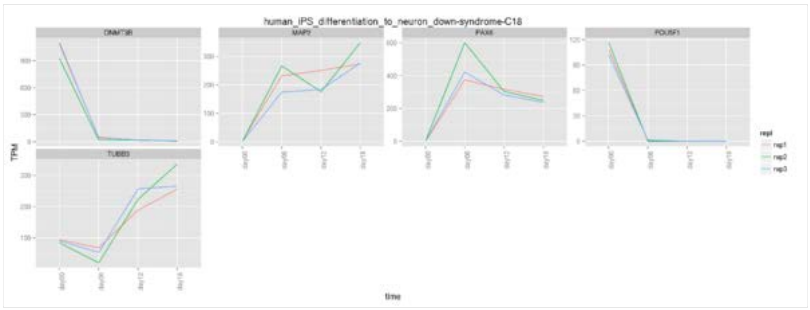

Figure 3B

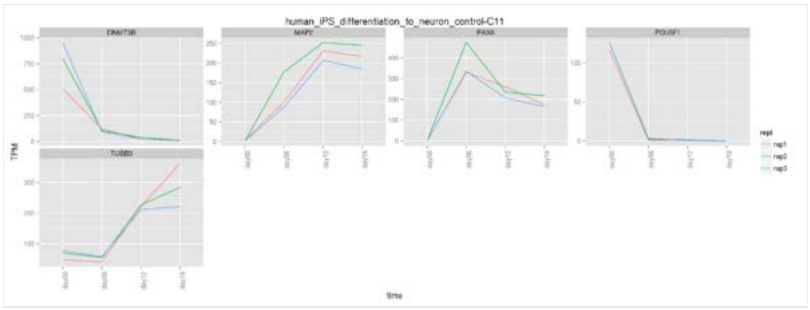

Figure 3C

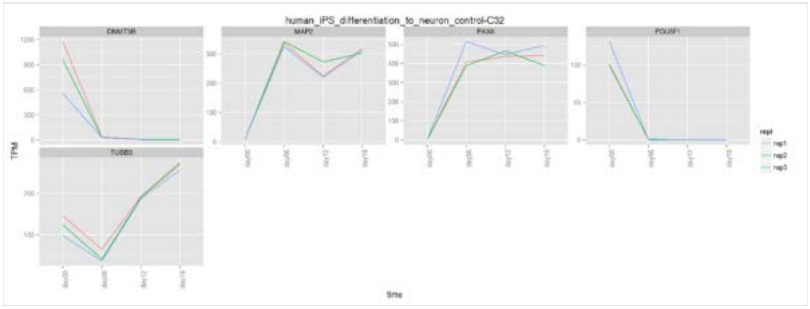

Figure 3D

Figure 3: CAGE analysis of DNMT3B, MAP2, PAX6, beta-III-tubulin and Oct4 expression by CAGE (TPM) in DS iPSC line C11 (A), DS iPSC line C18 (B), control iPSC line C11 (C) and control iPSc line C32 (D) during neuronal differentiation. Technical replicates shown in red, green and blue in each plot.

References

[1] Briggs, James A., et al. "Integration–Free Induced Pluripotent Stem Cells Model Genetic and Neural Developmental Features of Down Syndrome Etiology." Stem Cells 31.3 (2013): 467-478.

[2] Chambers, Stuart M., Christopher A. Fasano, Eirini P. Papapetrou, Mark Tomishima, Michel Sadelain, and Lorenz Studer. "Highly efficient neural conversion of human ES and iPS cells by dual inhibition of SMAD signaling." Nature biotechnology 27, no. 3 (2009): 275-280.

[3] Heins, Nico, Paolo Malatesta, Francesco Cecconi, Masato Nakafuku, Kerry Lee Tucker, Michael A. Hack, Prisca Chapouton, Yves-Alain Barde, and Magdalena Götz. "Glial cells generate neurons: the role of the transcription factor Pax6." Nature neuroscience 5, no. 4 (2002):

308-315.

[4] Reubinoff, Benjamin E., Pavel Itsykson, Tikva Turetsky, Martin F. Pera, Etti Reinhartz, Anna Itzik, and Tamir Ben-Hur. "Neural progenitors from human embryonic stem cells." Nature biotechnology 19, no. 12 (2001): 1134-1140.

[5] Pevny, Larysa H., Shantini Sockanathan, Marysia Placzek, and Robin Lovell-Badge. "A role for SOX1 in neural determination." Development 125, no. 10 (1998): 1967-1978.

[6] Gleeson, Joseph G., Peter T. Lin, Lisa A. Flanagan, and Christopher A. Walsh. "Doublecortin is a microtubule-associated protein and is expressed widely by migrating neurons." Neuron 23, no. 2 (1999): 257-271.

[7] Cheung, Martin, and James Briscoe. "Neural crest development is regulated by the transcription factor Sox9." Development 130, no. 23 (2003): 5681-5693.

[8] Ellis, Pam, B. Matthew Fagan, Scott T. Magness, Scott Hutton, Olena Taranova, Shigemi Hayashi, Andrew McMahon, Mahendra Rao, and Larysa Pevny. "SOX2, a persistent marker for multipotential neural stem cells derived from embryonic stem cells, the embryo or the adult." Developmental neuroscience 26, no. 2-4 (2005): 148-165.

[9] Sommer, Lukas, Nirao Shah, Mahendra Rao, and David J. Anderson. "The cellular function of MASH1 in autonomic neurogenesis." Neuron 15, no. 6 (1995): 1245-1258.

[10] Hu, Bao-Yang, Jason P. Weick, Junying Yu, Li-Xiang Ma, Xiao-Qing Zhang, James A. Thomson, and Su-Chun Zhang. "Neural differentiation of human induced pluripotent stem cells follows developmental principles but with variable potency." Proceedings of the National Academy of Sciences 107, no. 9 (2010): 4335-4340.

[11] Nichols, Jennifer, Branko Zevnik, Konstantinos Anastassiadis, Hitoshi Niwa, Daniela Klewe-Nebenius, Ian Chambers, Hans Schöler, and Austin Smith. "Formation of pluripotent stem cells in the mammalian embryo depends on the POU transcription factor Oct4." Cell 95, no. 3 (1998): 379-391.

[12] Okano, Masaki, Daphne W. Bell, Daniel A. Haber, and En Li. "DNA methyltransferases Dnmt3a and Dnmt3b are essential for de novo methylation and mammalian development." Cell 99, no. 3 (1999): 247-257.

Primary lymphatic endothelial cell response to vascular endothelial growth factor C (VEGFC)

Time course name: human_Lymphatic_Endothelial_cells_response_to_VEGFC

Sample provider: Michael Detmar

Introduction

The lymphatic vasculature plays a critical role in the maintenance of tissue fluid balance, the uptake of dietary fats and the immune response. Lymphatic vessels are also actively involved in pathological conditions, in particular in promoting cancer metastasis to lymph nodes and in controlling chronic inflammatory diseases (1, 2, 3, 4). The growth of new lymphatic vessels from pre-existing vasculature is called lymphangiogenesis. The main pathway regulating lymphangiogenesis is VEGF-C signaling via its receptor VEGFR-3 on lymphatic endothelial cells. Fully mature VEGF-C has affinity for VEGFR-2 which is also expressed on lymphatic endothelial cells (LEC) (5). A mutated version of VEGF-C, VEGF-C156S, in which cysteine 156 is replaced by a serine, specifically activates VEGFR-3 but not VEGFR-2 (6). Specific activation of VEGFR-3 by VEGF-C156S is sufficient to induce lymphangiogenesis, as demonstrated in K14-VEGF-C156S mice. Upon stimulation, the receptor dimerizes and is phosphorylated at several tyrosine residues. These phosphorylation sites activate several adaptor molecules along with further downstream mediators including JNK, ERK1/2, PI3K and PKB/AKT, ultimately leading phenotypic changes of LECs. However, the exact transcriptional mediators are not fully investigated yet. These transcription factors might be essential in mediating the effect of VEGF-C and could serve as potential therapeutic targets of the lymphatic endothelium.

Samples

We have used primary lymphatic endothelial cells, which have previously been isolated from human foreskin (7). Cells were cultured on collagen-coated culture dishes in EBM medium (Lonza) supplemented with 20% FBS (Life Technologies), 1x penicillin/streptomycin (Life Technologies), 2mM L-Glutamine (Life Technologies), 25 µg/ml cAMP (Sigma-Aldrich), and 10 µg/ml hydrocortisone (Sigma-Aldrich). For this study, we used cells isolated from 3 individual donors, at low passage numbers (<=6). Cells were seeded at 70% confluency and were starved in EBM + 0.2% BSA over night before stimulation with 1.5 µg/ml recombinant human VEGF-C156S (Kari Alitalo, University of Helsinki, Finland) for 0 min, 15 min, 30 min, 45 min, 60 min, 80 min, 100 min, 2 h, 2.5h, 3 h, 3.5 h, 4 h, 5 h, 6 h, 7 h, or 8 h (16 different time points). The 0 min time point of treatment served as a control for the other time points (Figure 1).

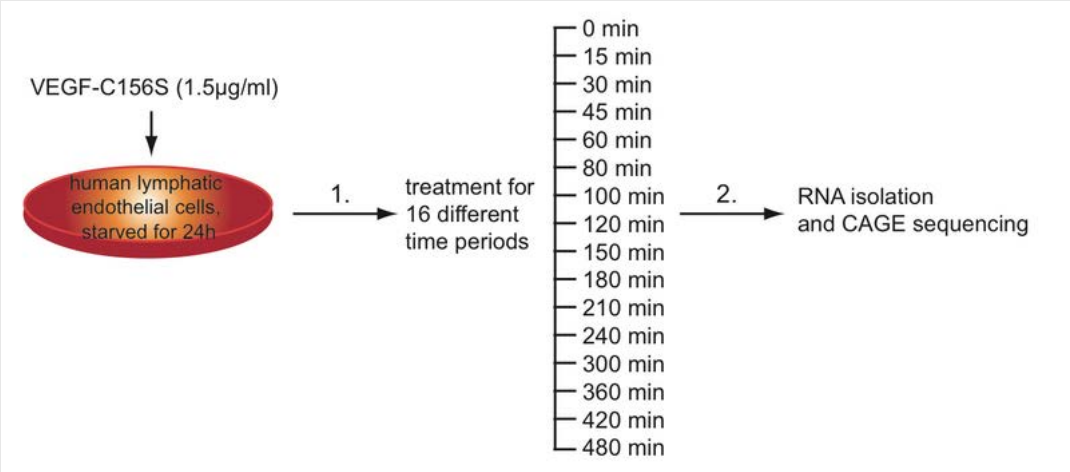

Figure 1: Schematic overview of the experimental procedure for the transcriptome analysis. Starved lymphatic endothelial cells (LECs) were treated with VEGF-C156S (1.5µg/ml) for various time periods from 0 min to 480 min. Treatment was terminated by adding TRIzol and isolating the RNA for CAGE sequencing.

Quality Control

Marker gene expression

Marker gene expression Key genes of interest behaved the same way in all three isolates. As expected, there was a rapid induction of the known VEGF-C target gene DLL4 (8), whereas SOX18, a master transcription factor of lymphatic cell identity, was robustly expressed over the whole time course, and was only mildly induced by VEGF-C156S (Figure 2).

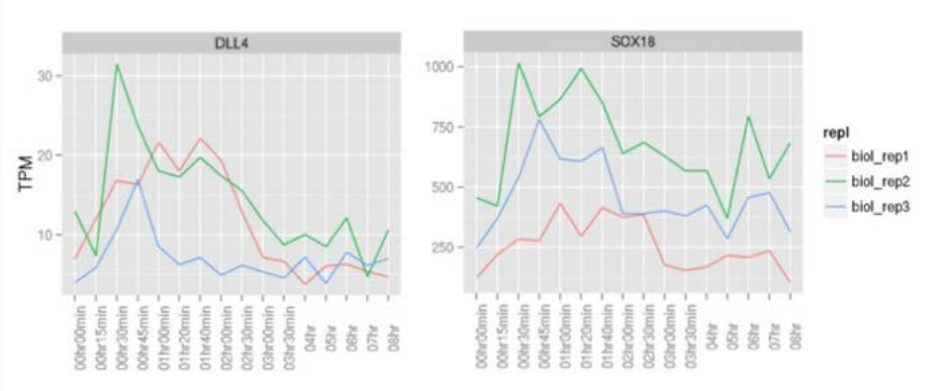

Figure 2: TPM expression profiles of individual replicates for the VEGF-C target genes Dll4 and SOX18. An early up-regulation of SOX18 and Dll4 can be observed after VEGF-C156S stimulation.

References

(1) Skobe et al. (2001) Nat Med, 7(2):192-8

(2) Hirakawa et al. (2007) Blood, 109(3):1010-7

(3) Hirakawa et al. (2005) J Exp Med, 201(7):1089-99

(4) Huggenberger et al. (2010) J Exp Med, 207(10):2255-69

(5) Joukov et al. (1997) EMBO J, 16:3898-3911

(6) Joukov et al. (1998) J Biol Chem, 273:65599-6602

(7) Hirakawa et al. (2003) Am J Pathol, 162(2):575-86

(8) Zheng et al. (2011) Blood, 118(4):1154-62

MCF7 response to Epidermal Growth Factor (EGF) and Heregulin (HRG)

Time course ID: human_MCF7_breast_cancer_cell_line_HRG and human_MCF7_breast_cancer_cell_line_EGF
Sample provider: Mariko Okada-Hatakeyama and Shigeyuki Magi

Introduction

ErbB receptor family plays a central role in cellular development, proliferation, differentiation and cell death. There are four members, ErbB1/EGFR, ErbB2, ErbB3 and ErbB4 receptors, belong to this family. Dysregulation of the receptors is highly associated with incidence of variety of cancers [1]. Once activated by growth factor binding, the receptor forms homo- and heterodimer and are trans-activated by tyrosine phosphorylation, transmits the phosphorylation signal to downstream kinase such as ERK and Akt, then those kinases activate/phosphorylate transcription factors such as ELK1, CREB, or SRF in nucleus to initiate gene expression.

In human breast cancer MCF-7 cells, the heregulin (HRG; a ErbB3/4 ligand) induces cell differentiation (accumulation of lipid droplets), while epidermal growth factor (EGF; an ErbB1/EGFR ligand) elicits cell proliferation after 5-14 days of the ligand stimulation.

These ligand-stimulated cells show similar time-course profiles in terms of signaling activity and immediate early gene (IEG) mRNA expression (up to 1.5 hours)[2,3]. However, analysis of delayed transcription (up to 72 hours) using qRT-PCR showed the significant expression of transcription factors (c-FOS, FRA-1 and FHL2) specific to HRG but not by EGF [4], suggesting the existence of unknown transcription machinery for cell differentiation during this time-course.

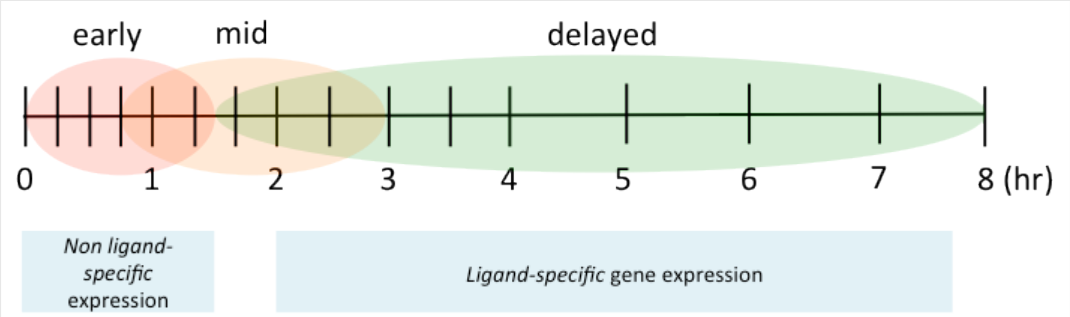

Figure 1: Approximate expression timing of early, mid, delayed response genes.

Samples

The MCF-7 human breast cancer cell line was obtained from American Type Culture Collection (ATCC) and maintained in DMEM (Gibco BRL, Githersburg, MD) supplemented with 10 % fetal bovine serum. Prior to growth hormone treatment, the cells were serum-starved for 16-24 hours, and then EGF (PeproTech House, London, England) or HRG-□176-246 (R&D Systems, Inc., Minneapolis, MN) was added. We prepared the EGF or HRG-stimulated time-course samples at 0 (non-treated), 15min, 30min, 45min, 60min, 80min, 100min, 2hr, 2.5hr, 3hr, 3.5hr, 4hr, 5hr, 6hr, 7hr and 8hr, to cover the early phase of cell differentiation and to cover early, mid and delayed gene expression. The all cell samples were snap frozen in liquid nitrogen and provided for RNA extraction for CAGE analysis.

MCF-7 cells were incubated in the absence or presence of growth factor in serum-free DMEM. Following cultivation for 14 days, cells were stained with Oil Red O to evaluate differentiation of the cells, which results in lipid droplets accumulation (The figures from Nagashima et al. JBC 2007 [2]).

Quality control

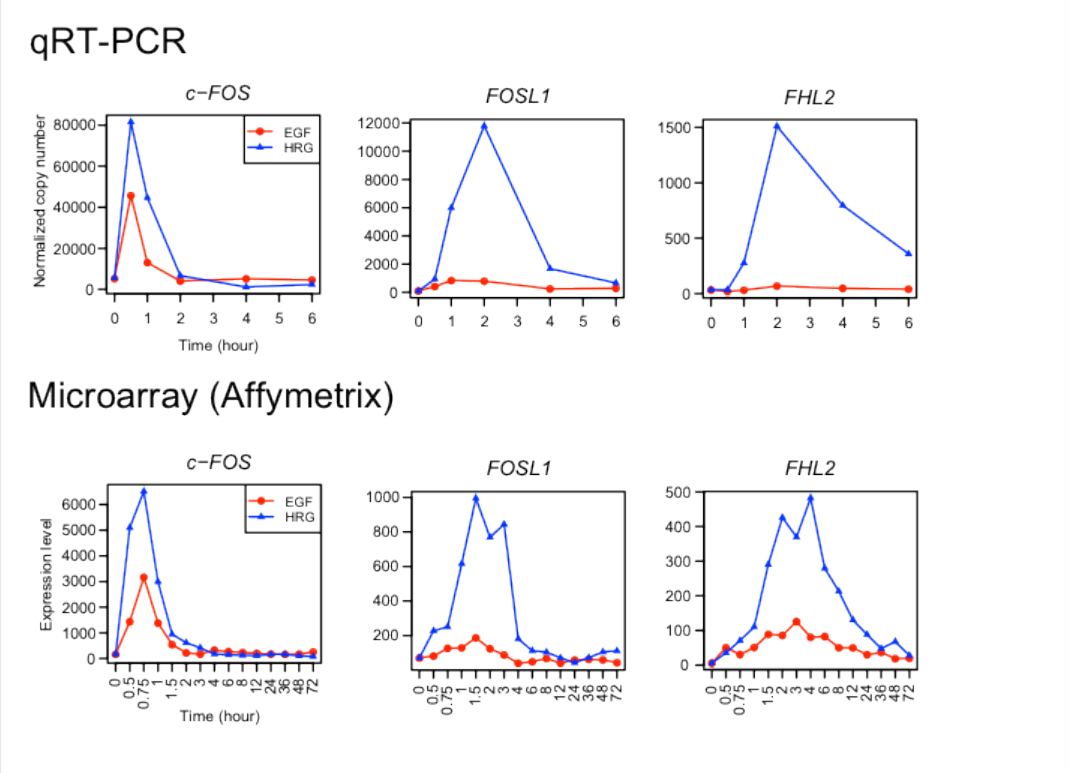

The mRNA expression of c-FOS, FOSL1 and FHL2 was significantly induced for HRG than EGF shown in the past study (The figures from Saeki et al BMC Genomics 2009[4]).

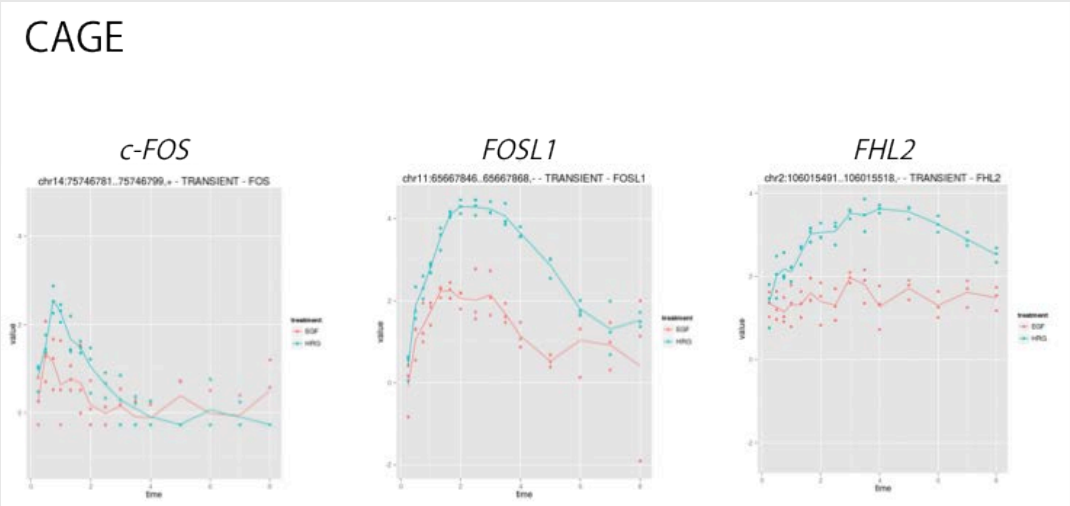

Time-course patterns the CAGE peaks of c-FOS, FOSL1, FHL2 obtained from current analysis was consistent with the mRNA expression data shown in above.

References

[1] Yarden Y1, Sliwkowski MX. Untangling the ErbB signalling network. Nat Rev Mol Cell Biol. 2, 127-137, 2001.

[2] Nagashima, et al. Quantitative transcriptional control of ErbB receptor signaling undergoes graded to biphasic response for cell differentiation. J. Biol. Chem. 282, 4045-4056, 2007.

[3] Nakakuki, et al. Ligand-specific c-Fos expression emerges from the spatiotemporal control of ErbB network dynamics. Cell 141, 884-896, 2010.

[4] Saeki, et al. Ligand-specific sequential regulation of transcription factors for differentiation of MCF-7 cells. BMC Genomics 10, 545, 2009.

The response of primary human monocyte-derived macrophages to lipopolysaccharide

Time course ID: human_Monocyte-derived_macrophages_response_to_LPS Sample provider: David Hume, Kenneth Baillie, Geoff Faulkner, Lynsey Fairbairn, Malcolm Fisher

Introduction

Macrophages are effector cells of the innate immune system. Their effector function is modulated in response to a wide range of stimuli. Amongst the most studied is lipopolysaccharide (LPS) or endotoxin, the major cell wall component of gram-negative microorganisms. LPS signals through the toll-like receptor 4 (TLR4) to initiate a cascade of transcriptional changes that have been analysed in detail in mice, and which involves waves of gene regulation starting within minutes and extending over 24-48 hours [1,2]. The earliest transcriptional responses, including key pro-inflammatory cytokines, involve the activation of transcriptional elongation from poised RNApolI complexes [3]. Recent studies in the mouse have identified many of the inducible enhancers activated in response to LPS, and the production of eRNAs from these elements [4,5]. However, there are many differences in the transcriptional responses of human and mouse macrophages to LPS [6], reflecting the impact of pathogen selection, and there is also significant variation between individuals. Accordingly, we have studied the response of macrophages from three different individuals.

Samples

Human monocytes were obtained from anonymised donors with approval of the Human Ethics Committee of the University of Edinburgh (8/9/09). 320mls of blood was extracted from healthy human volunteers and the mononuclear cell fraction was purified using Ficoll gradient centrifugation. The CD14-positive monocytes were purified from the mononuclear cell fraction using magnetic beads (Miltenyi Biotech), and cultured on bacteriological plastic plates in medium (RPMI-1640 plus 10% foetal calf serum) in recombinant human CSF1 (a gift from Chiron) at 100ng/ml. After 7 days the monocyte-derived macrophages were stimulated with 100ng/ml of salmonella R595 LPS. Samples were taken at 0 time, then 15, 30, 45, 60, 80, 100, 120, 150, 180, 210, 240 mins; then 5, 6, 7, 8, 10, 12, 14, 16, 18, 20, 22, 24, 36, 48 hours. Each time course was carried out on one preparation of cells from a single donor, and the precise temporal profile of gene expression varies somewhat between the three replicates. The system is comparable to more limited previous studies based upon microarrays and low-coverage CAGE analysis [6].

Quality control

In each case, the cells respond morphologically to LPS with increased spreading and vacuolation. The response to LPS can be detected through the early induction of classical inflammatory markers, TNF, IL6 and IL1B and late response genes such as IDO1 and CYP27B1 which are induced in human, but not in mouse macrophages [6]. The early response gene IFNB1, which acts in an autocrine manner to induce downstream target genes, is known to vary in its expression between individuals [7]. It was induced somewhat later in Donor 1 than in Donors 2 and 3, but the downstream response was evident in induction of known IFN targets such as MX1.

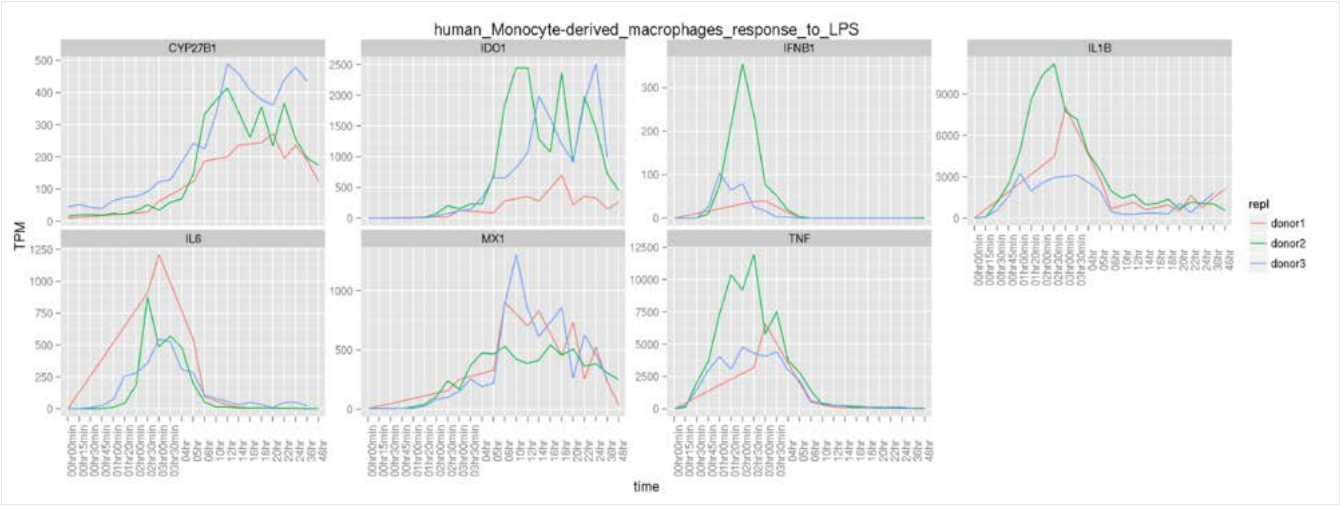

Figure 1: CAGE expression of marker genes in TPM

References

[1] PMID: 16688168

[2] PMID: 16698233

[3] PMID: 19859064

[4] PMID: 20206554

[5] PMID: 23332752

[6] PMID: 22451944

[7] PMID: 24604202

The response of primary human monocyte-derived macrophages to infection with Influenza A virus (Udorn strain)

Time course ID: human_Monocyte-derived_macrophages_response_to_udorn_influenza_infection Sample provider: David Hume, Kenneth Baillie, Andru Tomoiu

Introduction

The pathology of severe influenza virus infection involves a “cytokine storm”, not dissimilar to toxic shock initiated by severe bacterial infections. Although they are likely to be a major source of the cytokines in influenza virus pathology, macrophages are not generally regarded as permissive for infection by influenza virus infection. However, we and others [1] have noted that human macrophages grown in CSF1 become permissive for the virus. Like most viruses, influenza produces gene products, notably the NS1 protein, that interfere with the production of host defense proteins, notably interferon. This study aimed to compare the response of the human monocyte-derived macrophages to the response to bacterial endotoxin, assessed in parallel in this series.

Samples

Human monocytes were obtained from anonymised donors with approval of the Human Ethics Committee of the University of Edinburgh (8/9/09). 320mls of blood was extracted from healthy human volunteers and the mononuclear cell fraction was purified using Ficoll gradient centrifugation. The CD14-positive monocytes were purified from the mononuclear cell fraction using magnetic beads (Miltenyi Biotech), and cultured on bacteriological plastic plates in medium (RPMI-1640 plus 10% foetal calf serum) in recombinant human CSF1 (a gift from Chiron) at 100ng/ml. After 7 days the monocyte-derived macrophages were exposed to influenza. The influenza A (A/Udorn/72 (H3N2)) was propagated in MDCK cells as described [1]. Monocyte-derived macrophages were infected at a multiplicity of 5 PFU/cell for one hour in serum-free medium supplemented with TPCK-treated trypsin. The cells were then washed two times, and incubated for 0, 2 hrs, 7 hrs or 24 hrs. In this timecourse, the 0h timepoint is taken at the end of the incubation period. Mock-infected cells were also harvested at 0 time and 24 hours to control for the effect of protease and serum-free medium.

Quality control

In each case, the cells respond morphologically to influenza with increased spreading and vacuolation and at the later time point there was visual evidence of cell death. The infected cells produced active virus, which was quantified by plaque assay. They were also stained for viral NP protein using a fluorochrome-coupled antibody. The infected macrophages induce many proinflammatory cytokines in common with LPS. By contrast to macrophages responding to LPS, the influenza-infected cells displayed induction of multiple members of the interferon A family with substantial differences between the four replicates.

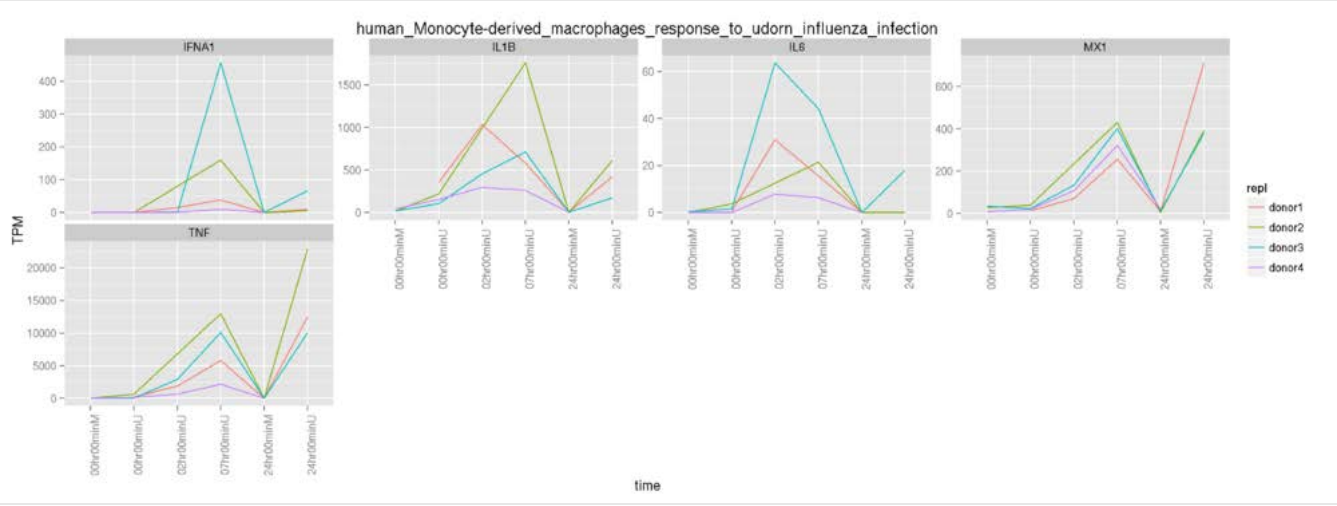

Figure 2: CAGE expression of marker genes in TPM.

References

[1] PMID: 22238612

Myotube differentiation

Time course ID: human_Myoblast_differentiation_to_myotubes
Sample provider: Beatrice Bodega and Valerio Orlando

Introduction

Differentiation of human primary skeletal myoblasts derived from healthy donors and patients affected by Duchenne Muscular Dystrophy

Skeletal muscle regenerates thanks to the proliferation of mononuclear myogenic precursor cells called myoblasts, which have the ability to fuse and become part of multinucleated myotubes, which at later mature into myofibers. The fusion of myoblasts is specific to skeletal muscle. Myoblasts express FGF receptor and IGF expression is increased during myoblast differentiation in culture. The human skeletal muscle myoblast culture is a convenient in vitro model for the study of cellular development and differentiation process. Duchenne muscular dystrophy (DMD) is a genetically well-defined disorder being associated with mutations in the dystrophin gene (1). Increasing evidence indicates that disruption of the dystrophin-associated protein complex (DAPC) at the sarcolemma affects not only the structure of muscle fibers, but impact global genome expression (coding and non coding transcripts) through deregulation of the nNOS-HDAC2 pathway (2,3)

Samples

Human primary cultures are derived directly from excised human tissue and cultured either as explants or after dissociation into a single cell suspension by enzyme digestion. Human primary myoblasts from healthy donors and DMD patients were obtained from Telethon BioBank, C. Besta Institute, Milan, Italy. All of the patients satisfied the accepted clinical criteria for DMD. They had undergone DNA diagnosis and were identified as carriers of specific exons deletions in the dystrophin gene. Details for individuals recruited for the study are listed in Table I. Muscle cells were cultured in DMEM supplemented with 20% FBS, human recombinant insulin (Sigma) 10 mg/ml, bFGF (Tebu-Bio) 25 ng/ml, EGF (Tebu-Bio) 10 ng/ml (proliferating medium), and induced to differentiate in DMEM supplemented with 2% horse serum (differentiating medium). For time course experiments, cells were harvested in proliferating condition (Myoblasts, Day 0) and at different days during the differentiation process (Myotubes, Day 1,2,3,4,6,8,10,12).

Individual	Specimen	Sex	Age at biopses	Mutation*
CN1	Quadriceps	F	3	-
CN2	Quadriceps	F	4	-
CN5	Quadriceps	M		
DMD1	Quadriceps	M	3	Δ 44
DMD3	Quadriceps	M	1	Δ 45
DMD5	Quadriceps	M	2	Δ 45 – 52

CN = control
DMD = Patients affected by Duchenne Muscular Distrophy
* Deletion (Δ) of specific exons in Dystrophin gene

Quality control

MyoD and Myogenin are transcription factors. MyoD is slightly upregulated (2-4 times), Myogenin is an early marker of differentiation, in general it is highly expressed in myocytes (day 1 to 4) before the fusion of these cells in polynucleated myotubes (day 4-5 to 12) when Myogenin expression is reduced. The class of Myosins genes are progressively upregulated for the entire process. Among genes that show the opposite trend you should find ID1, ID2 and ID3, known to inhibit differentiation, which are progressively repressed during differentiation.

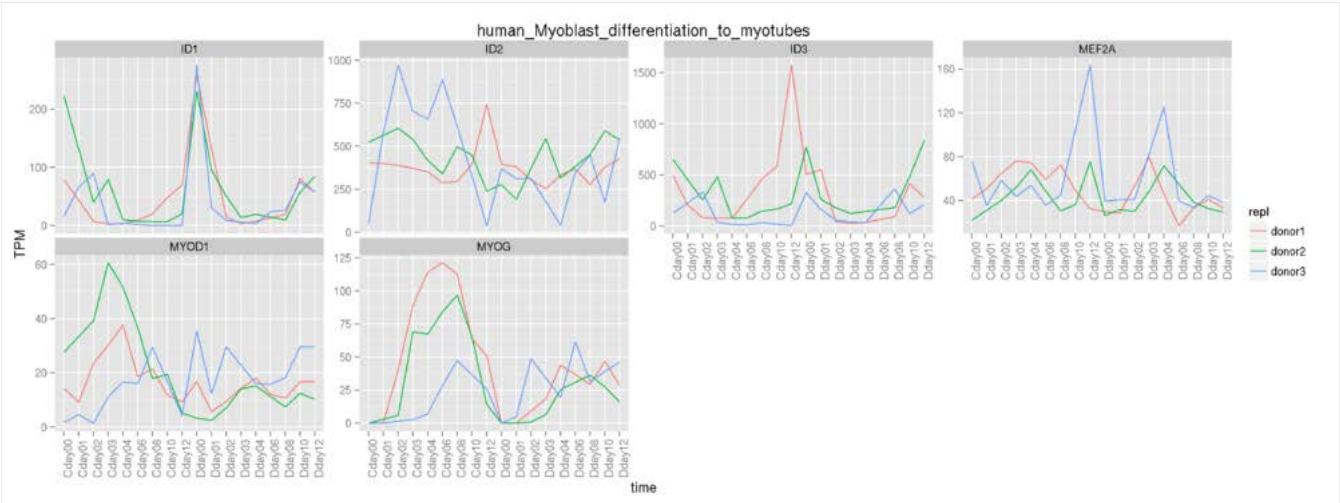

Figure 1: CAGE expression of marker genes in TPM.

References

[1] Davies, K. E. & Nowak, K. J. Molecular mechanisms of muscular dystrophies: old and new players. Nat Rev Mol Cell Biol 7, 762-773, (2006).

[2] Cacchiarelli, D. et al. MicroRNAs involved in molecular circuitries relevant for the Duchenne muscular dystrophy pathogenesis are controlled by the dystrophin/nNOS pathway. Cell Metab 12, 341-351, (2010). [3] Colussi, C. et al. Nitric oxide deficiency determines global chromatin changes in Duchenne muscular dystrophy. FASEB J 23, 2131-2141, (2009).

Rinderpest

Time course ID: human_rinderpest
Sample provider: Chieko Kai, Hiroki Sato, Misako Yoneda

Introduction

Morbilliviruses including measles virus and rinderpest virus (RPV) are one of the most important pathogens in their respective hosts. In particular, transient strong immunosuppression is the most characteristic feature. Morbillivirus infection induces cell-type-dependent immune responses. However, the molecular mechanisms have not been elucidated. Morbillivirus possesses two nonstructural accessory proteins, V and C. These proteins have been shown to inhibit interferon induction and signaling, although their full functions are unclear. To resolve the complexity and multidimensionality of virus–host interactions, we established recombinant RPV that lacked V and C proteins, and searched for the cell-type-specific transcriptional regulatory network after infection with the FANTOM5 time course analysis. Our study provides a new insight that an accessory protein is one of the virulence factors that define a cell-type-specific response of morbillivirus. This high-throughput experiment uncovers a novel host response against virus infection, and will be useful for understanding the whole picture of virus pathogenesis.

Samples

We used two major target cell type for RPV infection, a lymphoid cell line (COBL-a cells) and an epithelial cell line (HEK293 cells stably expressing receptor SLAM; 293SLAM cells) [1]. In addition, we established a reverse genetics for RPV-L strain, which is highly virulent against rabbit [2,3], and succeeded in generating recombinant RPV lacking C protein. Cells were infected with each RPV at a multiplicity of infection of 2, and were harvested at 6, 12, 24 and 48 h post infection. Three biological triplicates were performed.

Quality control

No marker genes are established yet. Infection, replication and growth of virus were verified by cytopathic effect of cells (formation of multinuclear giant cells).

References

[1] Measles virus induces cell-type specific changes in gene expression. Sato H1, Honma R, Yoneda M, Miura R, Tsukiyama-Kohara K, Ikeda F, Seki T, Watanabe S, Kai C. Virology. 2008 Jun 5;375(2):321-30. PMID:18374960

[2] Rinderpest virus H protein: role in determining host range in rabbits. Yoneda M, Bandyopadhyay SK, Shiotani M, Fujita K, Nuntaprasert A, Miura R, Baron MD, Barrett T, Kai C. J Gen Virol. 2002 Jun;83(Pt 6):1457-63. PMID:12029161

[3] Rinderpest virus phosphoprotein gene is a major determinant of species-specific pathogenicity. Yoneda M, Miura R, Barrett T, Tsukiyama-Kohara K, Kai C. J Virol. 2004 Jun;78(12):6676-81. PMID:15163758

Saos-2 osteosarcoma model of calcification/bone deposition

Time course ID: human_Saos-2_osteosarcoma
Sample provider: Kim Summers

Introduction

The formation of bone is a multi-stage process. It begins with mesenchymal cells committed to becoming cartilage. These cells condense into nodules and differentiate into chondrocytes which proliferate rapidly to form the template for the developing bone. They secrete a cartilege-specific extracellular matrix. blood vessels sinvade the cartilage structure. Mesenchymal precursors surrounding the cartilage cells then differentiate into osteoblasts which begin to form an extracelular matrix specific for bone. At the same time the chondrocytes within the osteoblast shell begin to die from apoptosis leaving a space that becomes the bone marrow. osteoblasts themselves become embedded into the bone matrix and differentiate further into osteocytes. Bone is constantly being remodelled by the action of osteoclasts, cells of the monocyte lineage that degrade the bone and osteoblasts on the surface which replace it with new bone. Thus the formation and maintenance of bone is a dynamic process.

During the formation of bone, osteoblasts lay down a matrix of hydroxyapatite, a mineral containing calciumand phosphorous which makes up to 50% of the weight of bone. this process of mineralisation can be simulated in vitro in cell cultures treated with chemicals to induce calcification. Many cell lines, primarily derived from osteosarcomas, can be induced to mineralise in this way, as can primary vascular smooth muscle cells. It is important to understand the process of mineralisation because formation of the bony skeleton is critical to the proper functioning of the vertebrate organism and because ectopic mineralisation can occur in genetic and environmental disease. For example, calcification is a key finding in forms of arterial disease including atherosclerosis.

Samples

In this study we used the human osteosarcoma cell line Saos-2. This line was first established from an osteosarcoma isolated from an 11 year old female patient in 1973 [1][2]. The line has been commonly used to study extracellular matrix and mechanical mechanisms in both expression and mineralisation studies [3] although the utility of Saos-2 as a human model system for normal osteoblast formation and function has been debated. Varying cellular morphology and proliferation has been observed [4], but Saos-2 demonstrates physiological levels of multiple osteoblastic markers including, osteocalcin (OC), bone sialoprotein (BSP) and decorin (DCN) [3]. In addition, active levels of alkaline phosphatase (ALPL) and the capacity to mineralize render Saos-2 a useful model system in the study of osteoblast function and ECM formation [5].

This experiment was designed to determine promoter specificity and gene expression patterns of key regulators early and late in the mineralization process using this human model system. To control for effects of serum cell proliferation and hyperconfluence we also submitted two control samples: mock-treated Saos-2 cells that had medium changes at the same time points but were not treated with BGP/ascorbic acid and MG63 osteosarcoma cells that were treated but failed ot mineralise. MG63 cells lack high levels of alkaline phosphatase and are not able to mineralise under these conditions, but they may respond to the signal by upregulating some required genes. [3][6].

The experiment was designed across 18 time points: 0, 15, 30, 45, 60, 80,100,120,150 and 180 minutes, 4, 8, and 24 hour as well as 4, 7, 14, 21, and 28 days following calcification induction. Cells were plated into 6 well plates (NUNC) or flasks (T25 or T75) at approximately 100,000 cells / well and mineralization was induced two days later with 50µg/ml ascorbic acid (Sigma) and 2.5mM ß-glycerophosphate (BGP) (Sigma) in medium with 10% serum. Medium was replaced with fresh medium including 10% serum and BGP/ascorbic acid every two to three days. All time point samples were processed for RNA at the same time relative to medium-change. RNA from the 18 time point samples were isolated through the following methods. The cells were lifted using 1x Trypsin-EDTA solution (Sigma) and RNA was isolated using the RNA Bee protocol (Ambisco). The sample RNA was quantified using a Nanodrop spectrophotometer (Nanodrop, USA). Three biological replicates were performed.

Quality control

Mineralization was verified using alizarin red staining of calcium at time point 0, 7, 14, 21 and 28 days. The cells were fixed with 4% paraformaldehyde (Sigma) for 10 minutes at room temperature, and rinsed with 1% PBS solution. The cells were stained using 1ml of 2% Alizarin Red (pH 4.2) for 5 minutes at room temperature. The wells were washed 3 times with dH20. The wells were extracted with 10% cetypyridium chloride and the extract used for quantification. The optical density was recorded using Multiskan ascent (Thermo) plate reader at a wavelength of 570nm.

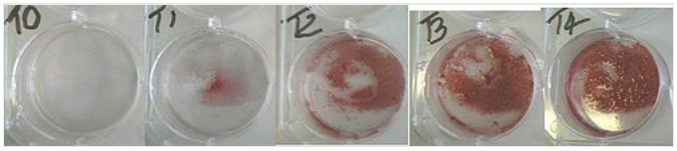

The image shows Saos-2 cells at 0, 1, 2, 3 and 4 weeks after initiation of calcification. Red staining shows calcium deposition.

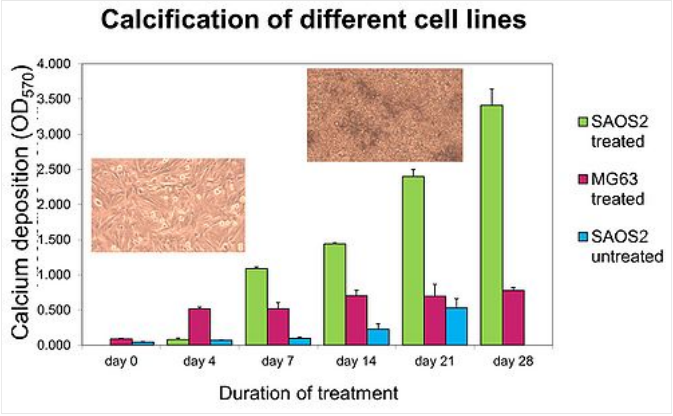

The graph shows quantification of calcium deposition in Saos-2 and MG63 cells treated with BGP and ascorbic acid and in untreated Saos-2 cells. Under treatment, Saos-2 cells deposit calcium in the matrix which MG63 do not and resemble the untreated Saos-2 cells. Pictures show the Saos-2 culture at 0 and 3 weeks where dark patches are caused by the deposition of calcium.

Marker gene expression

Key upregulated marker genes that indicate success of the mineralization:
COL1A2 [7], PHOSPHO1 [8], IFITM5 [9],SOST [10], DMP1 [10]

All these are markers of mineralisation in osteoblasts or the later stage osteocytes. All markers increased from Day1 or Day 4 and in general remained high for the remainder of the time course, indicating that calcification of the Saos-2 cultures involved induction of genes associated with miineralisation in vivo.

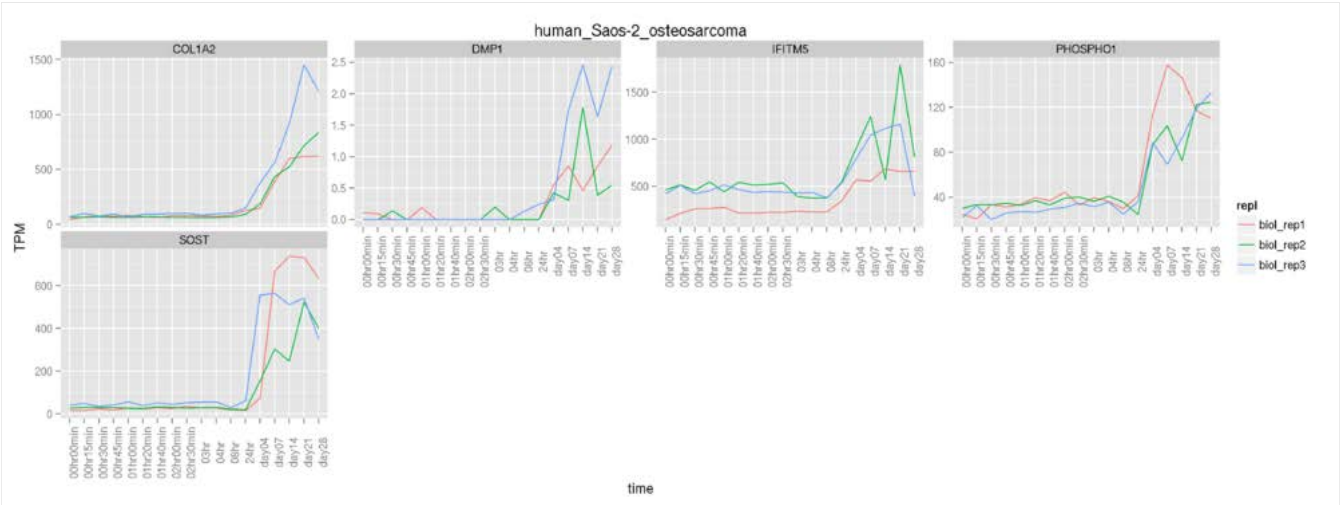

References

[1] Rodan S.B. et al., Characterizatin of a human osteosarcoma cell line (Saos-2) with osteoblastic properties. Cancer Res, 1987. 46(18): p. 4961-6.

[2] Fogh, J., J.M. Fogh, and T. Orfeo, One hundred and twenty-seven cultured human tumor cell lines producing tumors in nude mice. J Natl Cancer Inst, 1977. 59(1): p. 221-6.

[3] Pautke, C., et al., Characterization of osteosarcoma cell lines MG-63, Saos-2 and U-2 OS in comparison to human osteoblasts. Anticancer Res, 2004. 24(6): p. 3743-8.

[4] Boskey, A.L. and R. Roy, Cell culture systems for studies of bone and tooth mineralization. Chem Rev, 2008. 108(11): p. 4716-33.

[5] McQuillan, D.J., et al., Matrix Deposition by a Calcifying Human Osteogenic Sarcoma Cell Line (SAOS-2).Bone, April 1995. 16(4):p.415-26

[6] Billiau, A., et al., Human interferon: mass production in a newly established cell line, MG-63. Antimicrob Agents Chemother, 1977. 12(1): p. 11-5.

[7] Rodan, G.A., et al., Diversity of osteoblastic phenotype. Ciba Found Symp, 1988. 136: p. 78-91.

[8] Houston, B., et al., PHOSPHO1 - A novel phosphatase specifically expressed at sites of mineralisation in bone and cartilage. Bone, 2004. 34(4): p. 629-37.

[9] Moffatt P., et al., Bril. A novel bone-specific modulator of mineralization, J Bone Miner Res, 2008. 23:1497-508

[10] Bonewald, L.F., The amazing osteocyte. J Bone Miner Res, 2011. 26(2): p. 229-38.

Cerebellum development

Time course ID: mouse_cerebellum Sample provider: Thomas Ha, Peter Zhang, Dan Goldowitz

Introduction

Brain development requires intricately controlled expression of specific gene regulatory networks across time. Despite recent development in genomics technology, temporally-dependent large-scale transcriptome analyses across neural development are lacking. The cerebellum is a less complex, anatomically discrete and well-studied part of the mammalian brain that lends itself to such an analysis. To identify active transcription factor networks in developing mouse cerebellum, we analyzed the sequenced CAGE libraries from 12 time points across cerebellar development (embryonic days 11-18 at 24 hour intervals and every 72hrs until postnatal day 9).

Background

Brain development requires intricately controlled expression of specific gene regulatory networks across time. Despite recent development in genomics technology, temporally-dependent large-scale transcriptome analyses across neural development are lacking. The cerebellum is a less complex, anatomically discrete and well-studied part of the mammalian brain that lends itself to such an analysis. In cerebellum, the rhombic lip (RL) gives rise to the excitatory neurons of the cerebellum: first glutamatergic cerebellar nuclear neurons and then granule cell precursors and unipolar brush cells whereas the ventricular neuroepithelium gives rise to Purkinje cells and other GABAergic interneurons and cerebellar nuclear neurons. The key transcription factors Math1 and Pax6 are expressed in RL and the external germinal layer (EGL), and Ptf1a is expressed in the ventricular neuroepithelium. Cerebellar granule cells go through several epochs of development from their origins in the rhombic lip around E12.5 to the trans-migratory cells that establish the EGL, to the highly proliferative and then migratory population that produces the largest cohort of neurons in the brain. In spite of numerous studies on granule cell development, the understanding of the genetic underpinnings of the establishment of the EGL is limited. By taking advantage of FANTOM5 Cerebellr Developmental Time Course analysis, we plan to identify the transcriptional network controlling the development of cerebellum with primary focus on cerebellar granule cells.

Samples

Mice were housed in a room with 12/12 hr light/dark controlled environment. Embryos were obtained from timed pregnant females at midnight of the day when a vaginal plug was detected; this was considered embryonic day 0 (E0). Pregnant females were cervically dislocated and embryos were harvested from the uterus. The cerebellum was isolated from each embryo, pooled with littermates of like genotype, and snap-frozen in liquid nitrogen. 3-4 replicate pools of 3-10 whole cerebella samples were collected from 12 time points across cerebellar development (embryonic days 11-18 at 24 hour intervals and every 72hrs until postnatal day 9)

Laser capture microdissection (LCM), a technique that can isolate specific cell types of interest from regions of tissue, was used to obtain pure populations of granule cells from early-stages of mouse cerebellar development. Fresh frozen brain tissue from mouse embryo (aged E13, 15 and 18) were collected and cyro-sectioned into 8 µm thick sections. The sections were then stained with cresyl violet for histological identification of the EGL. Veritas automated LCM system (Arcturus Veritus) was used to capture cells from external granular layer with infrared laser. Finally, the captured cells were lysed and RNA from pure granule cell population was extracted.

Quality control

Bioanalyzer analysis was performed to check RNA quality. All RNA samples used for the time series achieved high RNA Integrity (RIN) Score. 34 out of 36 samples had RIN score of 9.7 or higher (10 being the best).

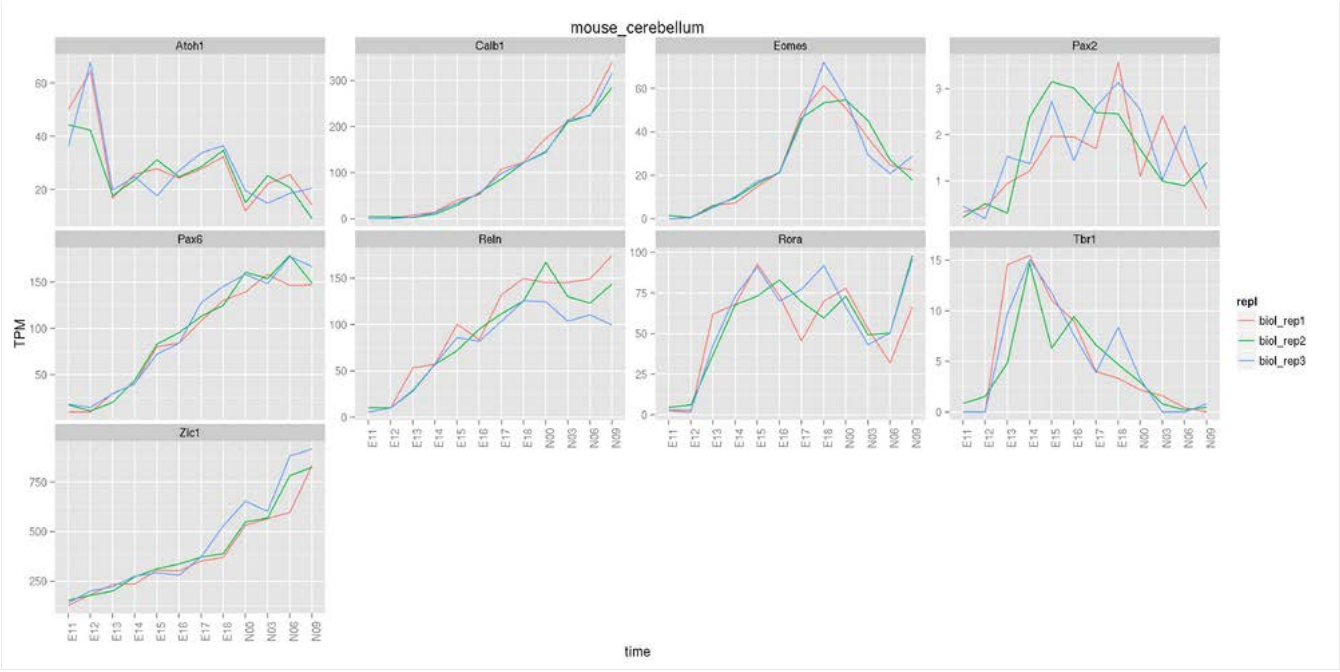

Figure 2: CAGE expression of marker genes in TPM.

References

[1] Ha TJ, Swanson D, Kirova R, Yeung J, Choi K, Tong Y, Chesler E, Goldowitz D (2012) Genome-wide microarray comparison reveals downstream genes of Pax6 in the developing mouse cerebellum. Euro J Neurosci (In Press).

[2] Tong Y, Ha TJ, Liu L, Nishimoto A, Reiner A, Goldowitz D (2011) Spatial and temporal requirements for huntingtin (Htt) in neuronal migration and survival during brain development. J Neurosci 31:14794-14799.

[3] Swanson, D.J., Y. Tong, and D. Goldowitz, Disruption of cerebellar granule cell development in the Pax6 mutant, Sey mouse. Brain Res Dev Brain Res, 2005. 160(2): p. 176-93.

[4] Goldowitz, D. and K. Hamre, The cells and molecules that make a cerebellum. Trends Neurosci, 1998. 21(9): p. 375-82.

T-cell differentiation

Time course ID: mouse_EBF_KO_HPCs_induced_to_T_cell
Sample provider: Horoshi Kawamoto and Tomokatsu Ikawa

Introduction

T cells are produced in the thymus. The earliest T cell progenitors in the thymus are not fully committed to the T cell lineage but retain potentials to give rise to other lineage cells, myeloid cells, dendritic cells and natural killer cells. The T cell progenitors gradually lose their potential and commit to the T cell lineage through interacting with thymic epithelial cells. However, the exact mechanisms are still poorly understood. Especially, the transcriptional networks controlling the T cell fate determination remain elusive because of the lack of suitable experimental systems. Here, we have established a coculture system using EBF1KO hematopoietic progenitor cells (HPCs) with the TSt-4/Delta-like (DLL) 1 stromal cells that support the T cell differentiation[1,2]. By applying this time course samples to CAGE analysis, we examined the gene regulatory networks underlying the T cell lineage commitment from multipotent hematopoietic progenitors.

Samples

We used EBF1KO HPCs, which were isolated from day 15 fetal livers of EBF1KO mice[1]. EBF1KO HPCs were maintained on TSt-4 stromal cells in IMDM (SIGMA) supplemented with 10% FBS (Life Technologies), 2-ME (5 x 10-5 M; Nacalai tesque), streptomycin (100mg/ml), penicillin (100U/ml) (both from Life Technologies), SCF, IL-7 and Flt3-L (all from R&D). 1 x 106 EBF1KO cells were transferred to TSt-4/DLL1 cells to induce T lineage differentiation. T lineage commitment was verified by the surface expression of CD117 and CD25 at day 6 of the culture. After inducing T lineage differentiation, we harvested the samples at 0 h, 0.5 h, 1 h, 2 h, 4 h, 6 h, 8 h, 10 h, 12 h, 24 h, 48 h, 72 h, 96 h, 120 h, 144 h of the culture. The 0 h time point serves as a control for the other time points (Figure 1).

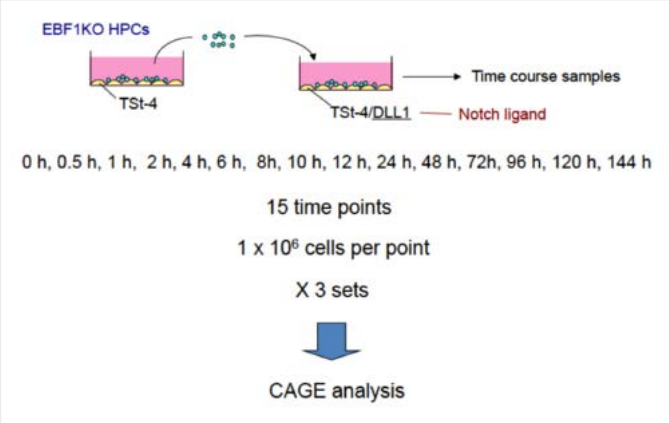

Figure 1: Schematic experimental procedure for the time course analysis. EBF1KO cells were transferred and cultured on the TSt-4/DLL1 stromal cells to induce T cell differentiation. The cells were harvested at each time point indicated in the figure. Total RNA was purified using miRNeasy Micro Kit (Qiagen) and served for CAGE analysis.

Quality control

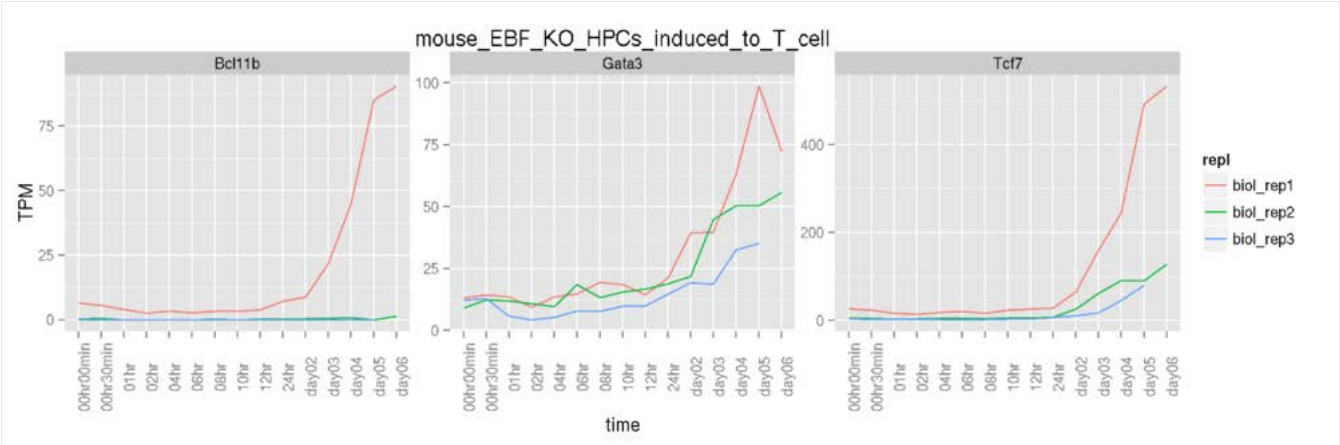

Figure 2: CAGE expression of marker genes in TPM.

References

[1] Lin YC, Jhunjhunwala S, Benner C, Heinz S, Welinder E, Mansson R, Sigvardsson M, Hagman J, Espinoza CA, Dutkowski J, Ideker T, Glass CK, Murre C. A global network of transcription factors, involving E2A, EBF1 and Foxo1, that orchestrates B cell fate. Nat Immunol. 11(7): 635-643, 2010

[2] Ikawa T, Hirose S, Masuda K, Kakugawa K, Satoh R, Shibano-Satoh A, Kominami R,Katsura Y, and Kawamoto H. An essential developmental checkpoint for production of the T cell lineage. Science 329: 93-96, 2010

ES series, ES-46C Dayo-4 Differentiation

Time course ID: mouse_ES-series
Sample provider: Carmelo Ferrai, Kelly Jane Morris, Ana Pombo

Introduction

The differentiation from Embryonic Stem (ES) cells to specialized cells is one of the most important fields of research in modern cell biology. Stem cell therapies promise cures for a plethora of complex diseases such as neurodegeneration. ES cells have the potential to differentiate into any of the 200 different cell types that make up higher organisms. A key challenge towards understanding the mechanisms by which the different programs of gene expression are established during differentiation is the development of stem cell therapies and differentiation protocols into specific cellular lineages. To this end, we are interested in understanding the mechanisms that control important developmental regulator genes in ES cells, and the dynamic changes that occur during early cell differentiation to neuronal lineages.

Samples

Cells were grown at 37°C in a 5% (v/v) CO2 incubator. Mouse ES cells (cell line ES-46C; ES cell line E14tg2a expressing GFP under Sox1 [1] were grown in GMEM medium (Invitrogen, # 21710025), supplemented with 10% (v/v) fetal calf serum (FCS; PAA, # A15-151), 2 U/ml LIF (Millipore, # ESG1107), 0.1 mM β-mercaptoethanol (Invitrogen, # 31350-010), 2 mM L-glutamine (Invitrogen, # 25030-024), 1 mM sodium pyruvate (Invitrogen, # 11360039), 1% penicillin-streptomycin (Invitrogen # 15140122), 1% MEM Non-Essential Amino Acids (Invitrogen, # 11140035) on gelatin-coated (0.1% (v/v)) Nunc T25 flasks. The medium was changed every day and cells were split every other day.

To investigate the early phases of neuronal commitment immediately after the cells exit from pluripotency, we followed a previously published protocol that provides a highly synchronous differentiation [2]. For the first time point, corresponding to day 0, 1.6x106 ES-46C cells were plated on gelatin-coated (0.1% (v/v)) Nunc 10 cm dishes in serum-free ESGRO Complete Clonal Grade Medium (Millipore, # SF001-500), containing 1U/ml LIF. For samples from day 1 to day 4, we started a monolayer protocol, where ES-46C cells are plated in serum-free medium ESGRO Complete Clonal Grade medium at high density (1.5x105 cells/cm2). After 24 hours, ES-46C cells were gently dissociated and plated onto 0.1% (v/v) gelatin-coated Nunc 10 cm dishes (1.6x106 cells per dish) in RHB-A media (StemCell Science Inc., # SCS-SF-NB-01). Media was changed every day.

All time point samples were processed for RNA at the same time relative to medium-change. After medium removal, TRIzol (Invitrogen, # 15596-018) was added directly to the dish and samples were treated following the manufacturer's instructions. Total RNA was treated with TURBO DNase I (Ambion, # AM1907) according to the manufacturer's instructions. Treated RNA (1 µg) was reverse transcribed with 50 ng random primers and 10 U reverse transcriptase (Superscript II kit, Invitrogen, # 18064-014) in a 20 µl reaction. The synthesized cDNA was diluted 1:10, and 2.5 µl used for qRT-PCR for quality control.

Quality control

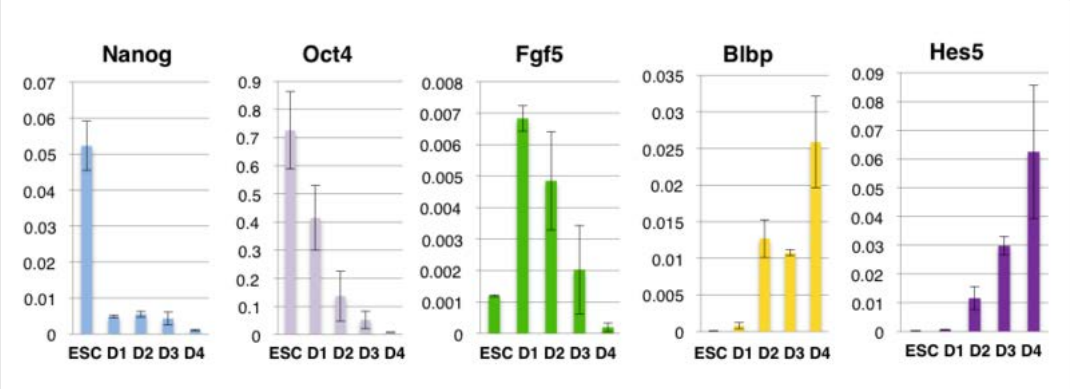

Figure 1: qRT-PCR expression of stage-specific markers

The time course was tested by qRT-PCR using stage-specific markers accordingly with [2]. QC shows that we achieved a synchronous and efficient progression of ES cells through the early differentiation steps into neuronal lineage. After 24 h, the levels of expression of the pluripotency marker Nanog is consistently decreased. Another relevant pluripotency marker, Oct4, is down-regulated at a slower rate, but shut down by day 4. A peak of expression of Fgf5, primitive ectoderm (PE) marker, shows an expected intervening state, before increasing

levels of Blbp and Hes5 from day 2 to day 4 confirms the switch from ES cell identity to neural precursor cells by day 4. Results are normalized to ß-actin, and represent the mean and standard deviations from two biological replicates.

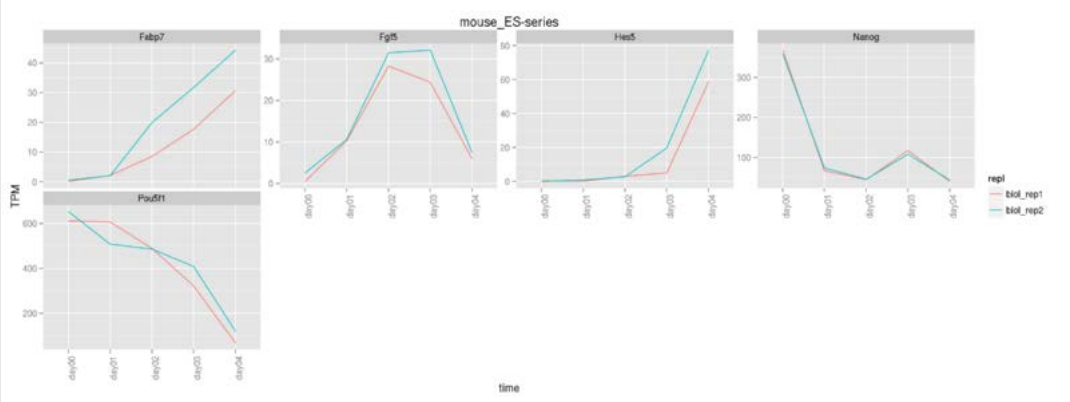

Figure 2: CAGE expression of marker genes in TPM.

References

[1] Conversion of embryonic stem cells into neuroectodermal precursors in adherent monoculture. Ying QL, Stavridis M, Griffiths D, Li M, Smith A. Nat Biotechnol. 2003 Feb;21(2):183-6. Epub 2003 Jan 13.

[2] Neural differentiation of embryonic stem cells in vitro: a road map to neurogenesis in the embryo. Abranches E, Silva M, Pradier L, Schulz H, Hummel O, Henrique D, Bekman E. PLoS One. 2009 Jul 21;4(7):e6286. doi: 10.1371/journal.pone.0006286.

J2E erythrocytic differentiation (EPO)

Time course ID: mouse_J2E
Sample provider: Peter Klinken and Louise Winteringham

Introduction

Erythropoietin (Epo) is the hormone, which regulates red blood cell production1. It is produced primarily in the kidney, and binds to Epo receptors (Epor) on the surface of immature erythroid cells in the bone marrow, thereby initiating the final stages of red cell maturation[1,2]. Following binding of Epo to its cognate receptor, a series of intracellular signaling cascades are activated, including stimulation of the JAK/STAT and ras/MAP kinase pathways[3,4]. This leads to enhanced cell division, followed by terminal differentiation which is characterized by the production of hemoglobin. In addition, morphological changes occur involving a reduction in cell size, nuclear condensation, and eventually extrusion of the nucleus to produce reticulocytes. Mature red blood cells (erythrocytes) containing large amounts of hemoglobin then circulate around the body transporting oxygen and carbon dioxide [5].

Samples

J2E model of Erythocytic differentiation

J2E cells are murine fetal liver cells that have been immortalised with the J2 retrovirus. J2E cells retain the capacity to respond to Epo by terminally differentiating and synthesizing hemoglobin6. The mouse J2E cell line responds to Epo by activating the JAK/STAT and ras/MAP kinase pathways7, as well as a novel Lyn-signaling cascade that we identified8. As a consequence of exposure to Epo, the cells undergo a burst of proliferation, followed by entry into the terminally differentiated state by synthesizing hemoglobin and changing morphologically9. These cells, therefore, provide a very good model for normal erythroid maturation in response to Epo.

J2E cells are maintained in DMEM (Gibco) 5% FCS (Bovogen Biologicals) at 370C and 5% CO2. Cell density is kept at 5-8 X105 cells/ml. Cells were induced with 5U/ml of Epo (Eprex®) (Jannsen). At least 1 X 107 cells were collected for RNA at 0min, 15min, 30min, 45min,1h, 1h 20min, 1h 40min, 2h, 2h 30min,3h, 3h 30min, 4h, 6h, 12h, 24h and 48h.

Key marker for differentiation

Enumeration of benzidine positive cells, as an indication of hemoglobin synthesis, was carried out to monitor differentiation. The time course of Epo-induced differentiation of J2E cells shows that hemoglobin production increases markedly 24-48h after stimulation (Figure 1).

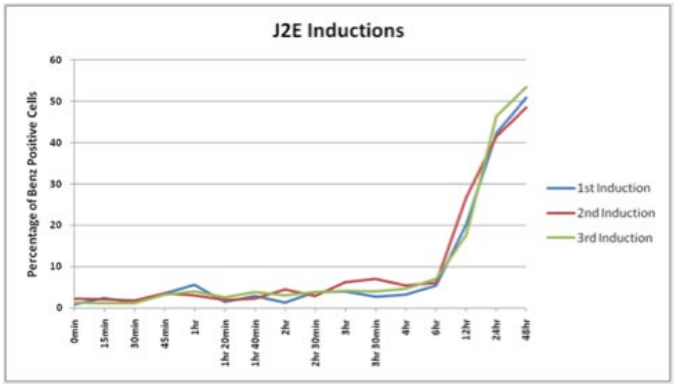

Figure 1. Benzidine positive cells were enumerated at each time point. Three biological replicates were analysed.

Quality control

Expression of the following genes was assessed to determine the validity of this cell line as a model of Epo-induced erythroid differentiation (Figure 2). All these genes are required for normal erythroid differentiation.

- Epor mediates epo-induced proliferation and differentiation [10]
- Alas2 is the rate limiting enzyme for the Heme biosynthesis pathway [11]
- Hbb-b1 hemoglobin, adult beta major chain required for oxygen transport [12]
- Gata-1 is an essential transcription factor for erythroid development [13, 14]
- Klf1 is a key transcriptional regulator for erythroid development [15]

- Nfe2 regulates erythroid maturation [16]

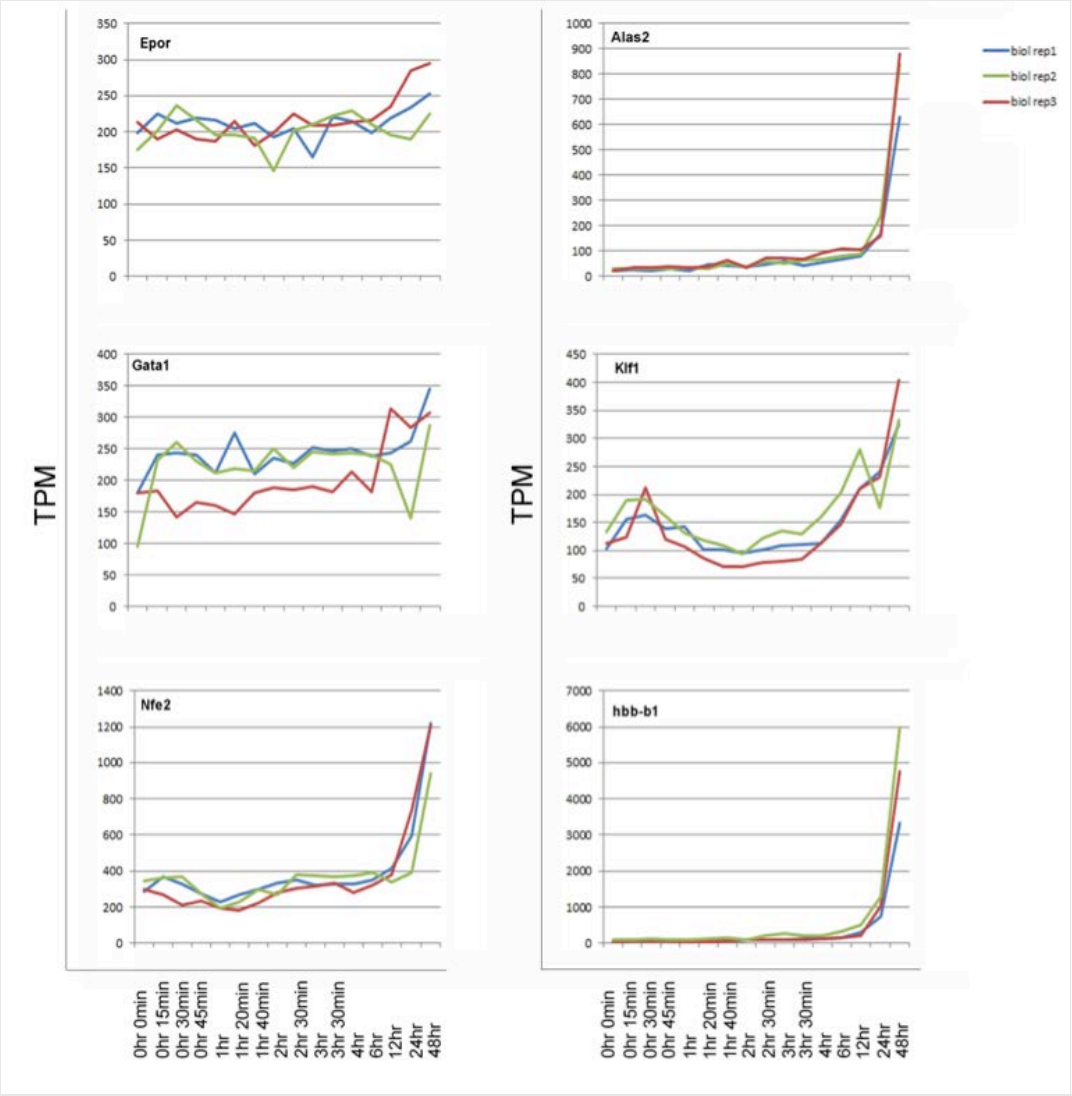

Figure 2. Expression of key genes associated with erythroid differentiation. TPM: Tags per million.

References

[1] Bunn HF. Erythropoietin. Cold Spring Harbor perspectives in medicine 2013; 3: a011619.

[2] Koury MJ, Koury ST, Bondurant MC, Graber SE. Correlation of the molecular and anatomical aspects of renal erythropoietin production. Contributions to nephrology 1989; 76: 24-29; discussion 30-22.

[3] Richmond TD, Chohan M, Barber DL. Turning cells red: signal transduction mediated by erythropoietin. Trends Cell Biol 2005; 15: 146-155.

[4] Ingley E. Integrating novel signaling pathways involved in erythropoiesis. IUBMB Life 2012; 64: 402-410.

[5] Palis J. Primitive and definitive erythropoiesis in mammals. Frontiers in physiology 2014; 5: 3.

[6] Klinken SP, Nicola NA, Johnson GR. In vitro-derived leukemic erythroid cell lines induced by a raf- and myc-containing retrovirus differentiate in response to erythropoietin. Proc Natl Acad Sci U S A 1988; 85: 8506-8510.

[7] Tilbrook PA, Bittorf T, Callus BA, Busfield SJ, Ingley E, Klinken SP. Regulation of the erythropoietin receptor and involvement of JAK2 in differentiation of J2E erythroid cells. Cell Growth Differ 1996; 7: 511-520.

[8] Tilbrook PA, Ingley E, Williams JH, Hibbs ML, Klinken SP. Lyn tyrosine kinase is essential for erythropoietin-induced differentiation of J2E erythroid cells. EMBO J 1997; 16: 1610-1619.

[9] Busfield SJ, Klinken SP. Erythropoietin-induced stimulation of differentiation and proliferation in J2E cells is not mimicked by chemical induction. Blood 1992; 80: 412-419.

[10] Lodish HF, Hilton DJ, Klingmuller U, Watowich SS, Wu H. The erythropoietin receptor: biogenesis, dimerization, and intracellular signal transduction. Cold Spring Harb Symp Quant Biol 1995; 60: 93-104.

[11] Meguro K, Igarashi K, Yamamoto M, Fujita H, Sassa S. The role of the erythroid-specific delta-aminolevulinate synthase gene expression in erythroid heme synthesis. Blood 1995; 86: 940-948.

[12] Stamatoyannopoulos G. Control of globin gene expression during development and erythroid differentiation. Exp Hematol 2005; 33: 259-271.

[13] Tsai SF, Martin DI, Zon LI, D'Andrea AD, Wong GG, Orkin SH. Cloning of cDNA for the major DNA-binding protein of the erythroid lineage through expression in mammalian cells. Nature 1989; 339: 446-451.

[14] Whitelaw E, Tsai SF, Hogben P, Orkin SH. Regulated expression of globin chains and the erythroid transcription factor GATA-1 during erythropoiesis in the developing mouse. Mol Cell Biol 1990; 10: 6596-6606.

[15] Miller IJ, Bieker JJ. A novel, erythroid cell-specific murine transcription factor that binds to the CACCC element and is related to the Kruppel family of nuclear proteins. Mol Cell Biol 1993; 13: 2776-2786.

[16] Andrews NC, Erdjument-Bromage H, Davidson MB, Tempst P, Orkin SH. Erythroid transcription factor NF-E2 is a haematopoietic-specific basic- leucine zipper protein. Nature 1993; 362: 722-728.

BMDM TB infection

Time course ID: mouse_macrophage_TB_infection_IFNg, mouse_macrophage_TB_infection_IL13, mouse_macrophage_TB_infection_IL4, mouse_macrophage_TB_infection_IL4-IL13

Sample provider: Frank Brombacher, Reto Guler, Sugata Roy, Harukazu Suzuki.

The present study was designed uncover the macrophage transcriptom during IFN-g, IL-4 or IL-13 macrophage activation (classical versus alternative), to discriminate differences between IL-4 and IL-13-induced alternative macrophage activation and to uncover the transcriptom dynamics during infection with Mycobacterium tuberculosis HN878 by high throughput transcriptome analysis method, CAGE (cap analysis of gene expression). Helicos CAGE analysis will enable us to construct promoter-based networks of transcriptional regulation in a time course during macrophage activation and during infection in classical and alternative activated macrophages.

Samples

Experimental Design

The experiment was designed across 11 time points: 0, 2, 4, 6, 12, 24, 28, 36, 48, 72, 120 hours after macrophage stimulation and 4, 12, 24, 48, 72 hours after infection. Bone marrow derived macrophages were generated from 8-12 week old BALB/c male mice (n = 5-10). After euthanasia, the tibias and femurs aseptically removed and the bone marrow was flushed out with cold DMEM supplemented with 10% FCS and 100U/ml penicillin G, 100µg/ml streptomycin. Bone marrow cells from several animals (n=5-10) were pooled and were cultured for 10 days at 37°C under 5% CO2 in PLUTNIK differentiation medium (DMEM supplemented with 10% FCS, 5% Horse serum, 100U/ml penicillin G, 100µg/ml streptomycin 2mML-glutamine, 1mM sodium poyruvate, 50 µM mercaptoethanol and 30% L929 conditioned medium as a source of M-CSF. On day 10, cells (now mature BMDM) were harvested and plated in 6-well TC grade dishes. Each well was seeded with 5x10e6 BMDMs in DMEM supplemented with 10% FCS and 100U/ml penicillin G, 100µg/ml streptomycin in the presence or absence activators (100U/ml IL-4 and/or 100U/ml IL-13 or 100U/ml IFNg). After 24 hours of stimulation, the BMDMs were left alone or infected with live logarithmic phase Mycobacterium tuberculosis (MTB) HN878 at a MOI 5:1 (bacilli:macrophage). Thereafter at specific time points the culture supernatants was removed , aliquoted and stored at -80 degree C until further analysis (.e.g. measure production of cytokines, chemokines and iNOS). The BMDMs were lyzed in situ in the well in 1 ml of Qiazol Lysis Solution (Qiagen) and the lysates stored at -80 degree C until further extraction and analysis at RIKEN. The experiment was done in parallel using 96-well TC plates where 1x105 BMDMs were plated in triplicate and treated as above for the 6-well plates. At the specific time points, the culture supernatants was collected and used for measuring the producton iNOS. The BMDMs were lyzed in 0.1% Triton X100 and cell lysate used for measuring (i) the Arginase 1 activity and (ii) CFU load in the cell lysates. Once all the samples were collected, the Qiazol cell lysates were sent to RIKEN, where the total RNA was isolated using the miRNeasy Mini kit (QIAGEN) and fully analysed. The total RNA was quantified using a NanoDrop spectrophotometer (NanoDrop, USA). The quality and concentration of total RNA was confirmed using the BioAnalyzer (Agilent 2100 BioAnalyzer). The sample quality was checked by performing quatitative RT-PCR for some of the important marker genes of classically activated macrophages (iNOS, IL-1b, TNFa) and alternatively activated macrophages (Arg1, Ym1, IL-10). Three biological replicates were performed.

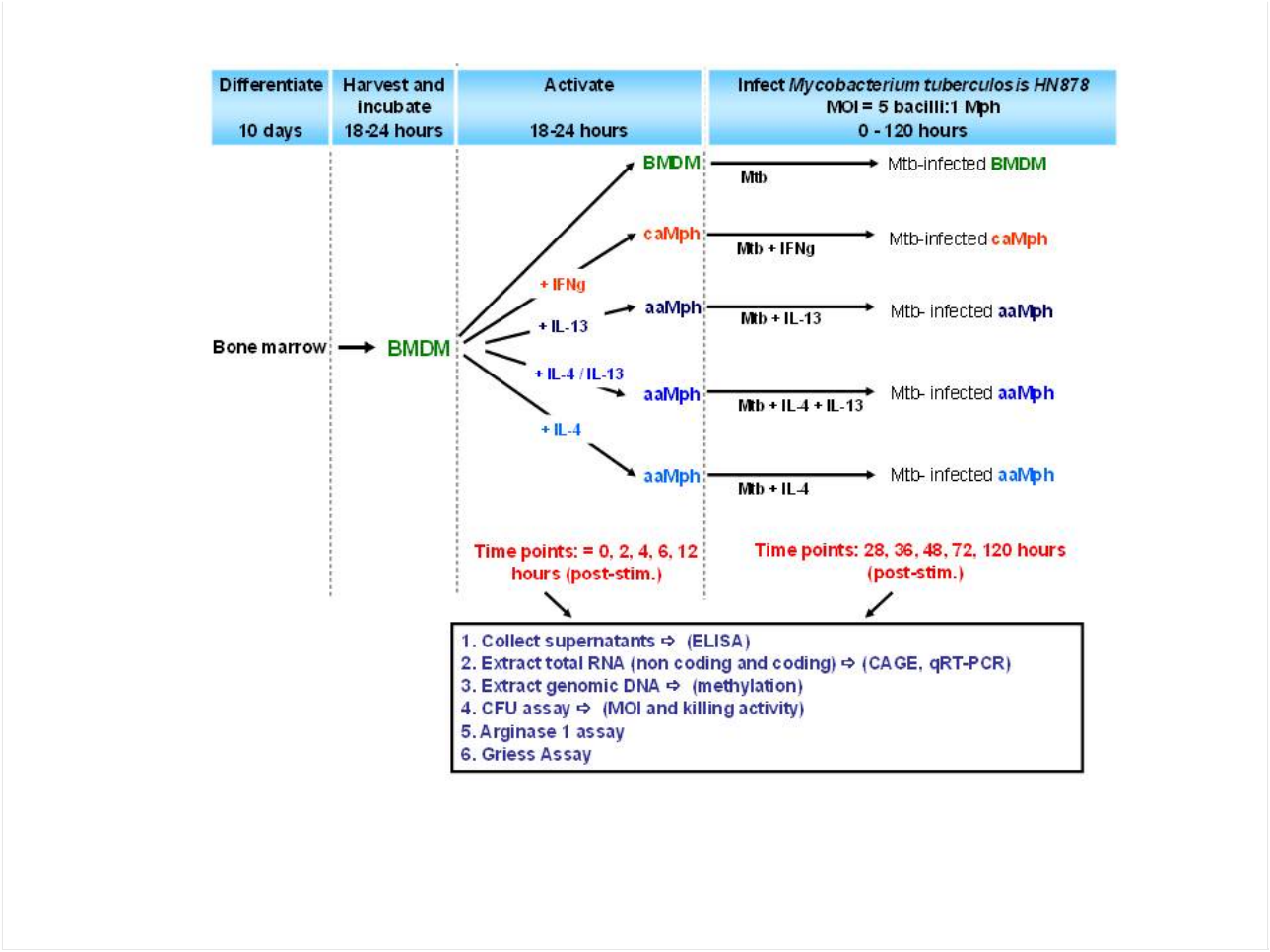

Figure 1. Schematic of experimental design

Bone marrow derived macrophages were generated from 8-12 week old BALB/c male mice, harvested and left alone or stimulated with activators to drive polarization to caMphs (100U/ml IFNg) or aaMphs (100U/ml IL-4 and/or 100U/ml IL-13). After 24 hours of stimulation, the BMDMs were left alone or infected with live logarithmic phase Mycobacterium tuberculosis (MTB) Beijing strain HN878 at a MOI 5:1 (bacilli : macrophage). Thereafter at specific time points, culture supernatants were analyzed to quantify the production of cytokines, chemokines and iNOS, and the BMDMs were lyzed in 1 ml of Qiazol Lysis Solution (Qiagen) and the DNA and total RNA (including microRNAs, long non-coding RNAs etc) extracted. The epigenomic footprint of the cells will be studied by analysing the genomic DNA methylation patterns by bisulifte sequencing; and the RNA will be used for RNAseq (microRNA and non-coding long RNA), CAGE analysis (promoter and gene expression) and qRT-PCR (confirmation).

Quality control

These are the well established marker of classical and alternative activation. The role of these genes were evaluated in human and mouse model of macrophage activation.

Marker gene Expression from CAGE data

Classical Marker genes

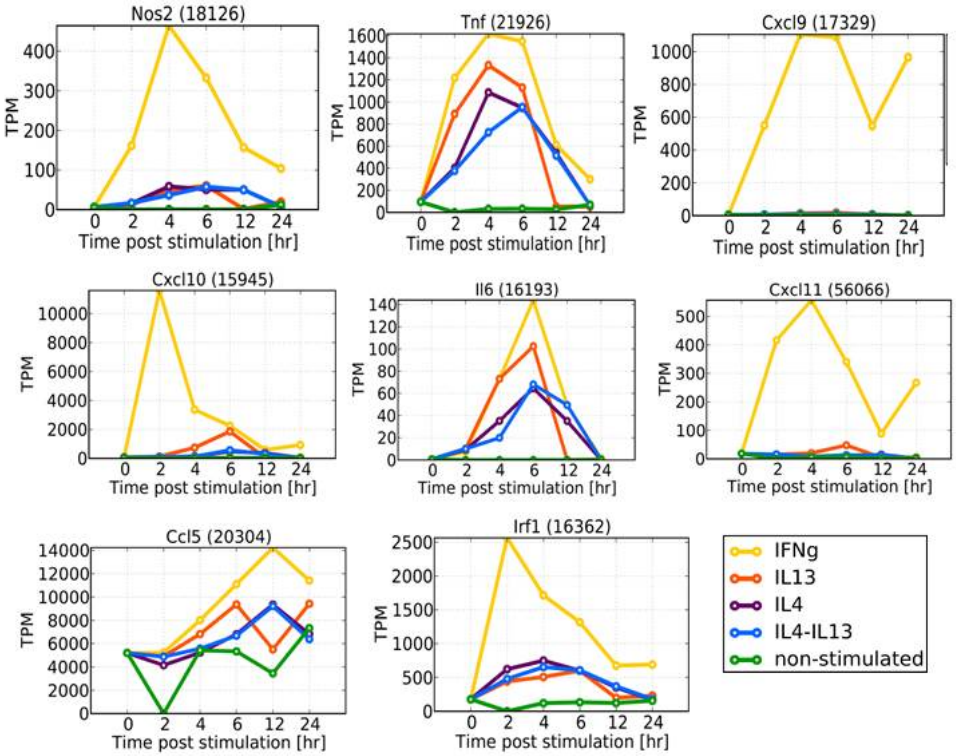

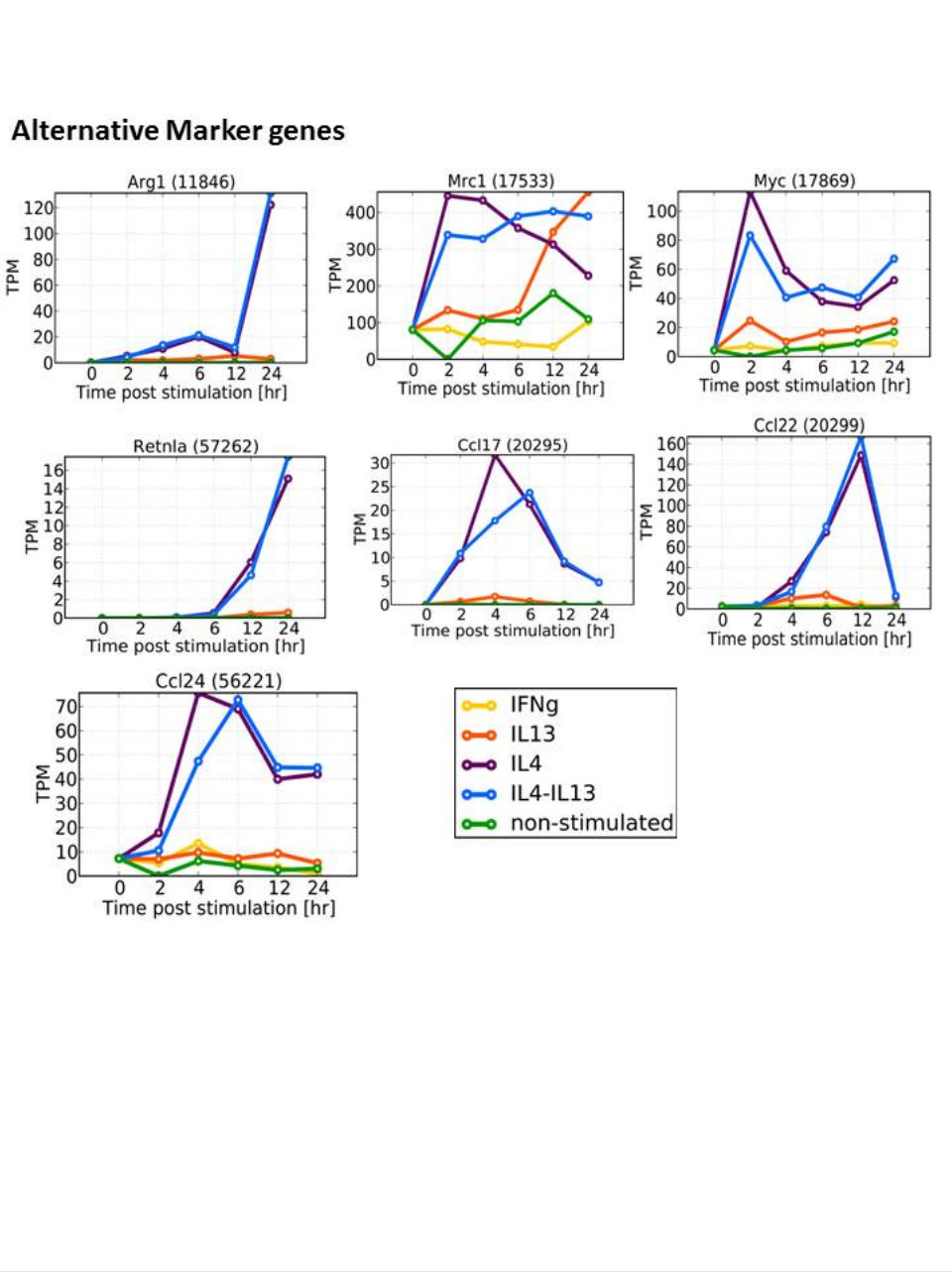

	Gene name	Referenced in (PMIDs)
Classical Activation	Nos2	1531844, 21441450, 15036034, 12215441, 10072066, 16920488
	Tnf	15070757, 20059482,16920488, 21607943, 21240265, 20717022
	CXCL9	20692533,16920488, 14734716, 19819674, 21607943, 20717022
	CXCL10	1531844, 11907072,16920488, 14734716, 19105661, 19819674.
	CXCL11	20692533,19819674, 23029029, 22666284
	CCL5	23223452,16920488, 20729857, 9822252, 18350541, 19841166
	IL-6	16840796,15036034, 12215441, 10072066, 16920488, 11927645
	Irf1	Ref in: 9822252, DOI:10.1016/j.cellimm.2013.01.010
Alternative activation	Arginase-1	12098359;15036034, 12511873, 10072066, 12215441, 16920488
	CCL22	23275605 ,15036034, 12511873, 10704248, 16920488, 14734716
	CCL17	23275605,15036034, 12511873, 16920488, 14734716, 19105661
	Ccl24	23275605, 20692533,16920488, 19105661, 20729857, 18350541
	Relmα	21093321, 19029990, 12554797, 19105661; 17082649; 15142530
	MYC	22067385
	Mrc1	18250477,12401408, 15530839, 19029990, 10072066, 19105661

References

[1] Bronte, V. and P. Zanovello (2005). "Regulation of immune responses by L-arginine metabolism." Nat Rev Immunol 5(8): 641-54.

[2] Chacon-Salinas, R., J. Serafin-Lopez, et al. (2005). "Differential pattern of cytokine expression by macrophages infected in vitro with

different Mycobacterium tuberculosis genotypes." Clin Exp Immunol 140(3): 443-9.

[3] Davis, A. S., I. Vergne, et al. (2007). "Mechanism of inducible nitric oxide synthase exclusion from mycobacterial phagosomes." PLoS Pathog 3(12): e186.

[4] Ehrt, S., D. Schnappinger, et al. (2001). "Reprogramming of the macrophage transcriptome in response to interferon-gamma and Mycobacterium tuberculosis: signaling roles of nitric oxide synthase-2 and phagocyte oxidase." J Exp Med 194(8): 1123-40.

[5] El Kasmi, K. C., J. E. Qualls, et al. (2008). "Toll-like receptor-induced arginase 1 in macrophages thwarts effective immunity against intracellular pathogens." Nat Immunol 9(12): 1399-406.

[6] Raju, B., Y. Hoshino, et al. (2008). "Gene expression profiles of bronchoalveolar cells in pulmonary TB." Tuberculosis (Edinb) 88(1): 39-51.

[7] Varin, A., S. Mukhopadhyay, et al. "Alternative activation of macrophages by IL-4 impairs phagocytosis of pathogens but potentiates microbial-induced signalling and cytokine secretion." Blood 115(2): 353-62.

ST2 mesenchymal stem cell differentiation to adipocyte and osteoblast

Time course ID: mouse_ST2_adipocytes, mouse_ST2_ osteoblasts
Sample provider: Yasushi Okazaki, Yutaka Nakachi and Yosuke Mizuno

Introduction

Senile osteoporosis is the most common metabolic bone disease. This disease is often accompanied by increasing adipocytes in bone marrow tissues [1]. The ectopic adipocytes differentiation following bone loss seems to be caused by unbalanced differentiation of mesenchymal stem cells (MSCs) [2]. Although several differentiation regulators of MSCs have already been reported, little is known about the regulatory dynamics of bi-directional adipocytes/osteoblasts differentiation.

To uncover the complex mechanism of osteoporosis and metabolic disease, we performed a variety of genome-wide analyses about gene expression and regulation that could influence adipocytes/osteoblasts differentiation from mouse ST2 cells (bone marrow-derived stromal cell line) [3,4]. In particular, we focused on the differentiation-specific non-cording RNAs and antisense transcripts as the novel regulator candidates of adipocytes/osteoblasts differentiation.

Sample

Cell line:
ST2 cells were obtained from RIKEN BioResource Center (BRC, Tsukuba, Japan). These cell line is bone marrow-derived stromal cell line. ST2 differentiated most efficiently into both osteoblasts and adipocytes [3].

Cell culture:
ST2 cells were cultured according to the protocols supplied by BRC (RPMI1640 supplemented with 10% fetal bovine serum) [4].

Differentiation induction:

Adipocyte differentation:
Adipogenic differentiation was induced by changing the medium to differentiation medium supplemented with 10% fetal bovine serum (FBS), 0.5 mM 3-isobutyl-1-methlxanthine, 0.25 mM dexamethasone, and insulin-transferrin-selenium-X supplement containing 5 mg/ml of insulin (Invitrogen, Carlsbad, CA) and 1 mM rosiglitazone. After 48 hr, the differentiation medium was replaced with conditional culture medium supplemented with 10% FBS [3]. Pre-conditioned medium which was originally same as culure medium, was carried by parallel culturing of ST2, to avoid the perturbation by "medium-change" shock as soon as possible.

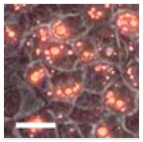

Figure 1. Histological staining of ST2 cells using Nile Red staining during adipocyte differentiation.
The number of Nile Red stained lipid droplets increased in ST2 cell (4 days after adipocyte induction). Bar: 100 μm.

Osteoblast differentiation:
Osteogenic differentiation was induced by changing the medium every three days to culture medium supplemented with 100 ng/ml of bone morphogenetic protein 4 (BMP4, R&D Systems, Mineapolis, MN) [3]. Pre-conditioned medium which was originally same as culure medium, was carried by parallel culturing of ST2, to avoid the perturbation by "medium-change" shock as soon as possible.

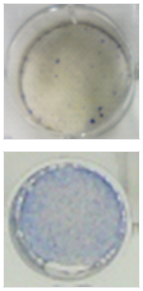

Figure 2. ALP staining of ST2 cells for 0, 6 and 20 days after osteoblast induction.
The ALP activity of ST2 cells (right, 20 days) were more prominently increased in the presence of BMP4 than 0 day (left).

Sampling:
ST2 cells are sampled during adipocyte or osteoblast differentiation (15min, 30min, 1-3hr, 6,12,18,24,36,48hr, 3-6day) and non-treatment control (2 points; 0,6day).

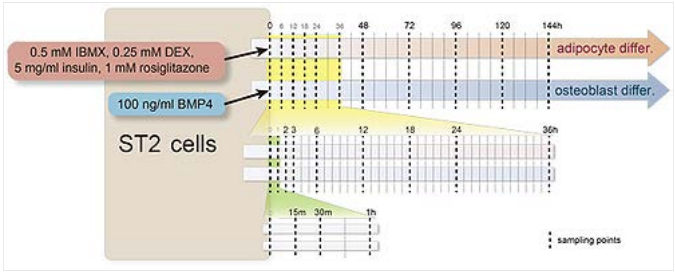

Figure 3. Sampling points for ST2 time-course CAGE data

Quality control

Marker gene expression:

Adipocyte differentation, hCAGE:

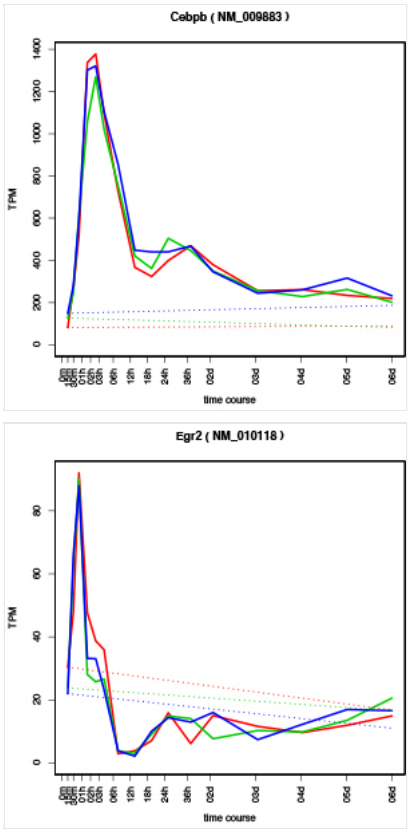

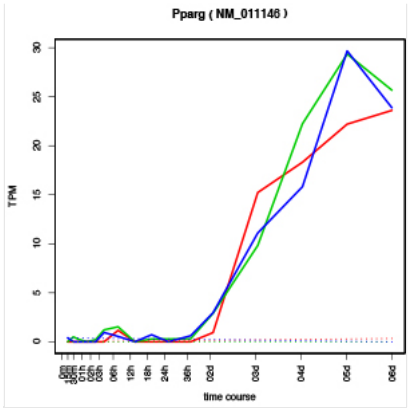
Pparg (NM_011146)
TPM
time course


rep1
rep2
rep3
rep1,
no induction
rep2,
no induction
rep3,
no induction

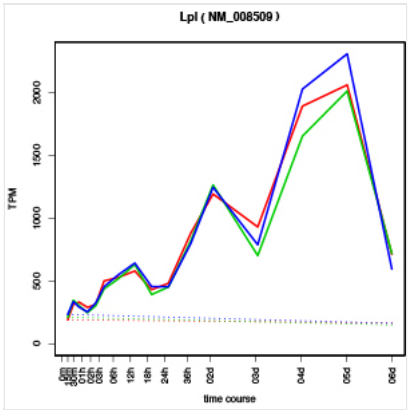
Lpl (NM_008509)
TPM
time course

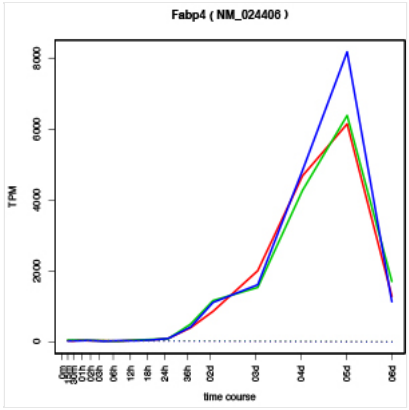
Fabp4 (NM_024406)
TPM
time course

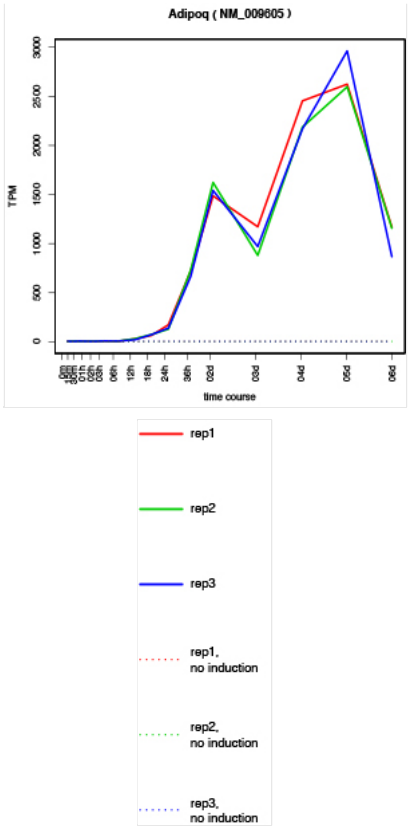

Figure 3. Gene expression (TPM) of key regulators (*Cebpb*, *Erg2*, *Pparg*) and differentiation markers (*Lpl*, *Fabp4*, *adipoq*).

Osteoblast differentiation, hCAGE:

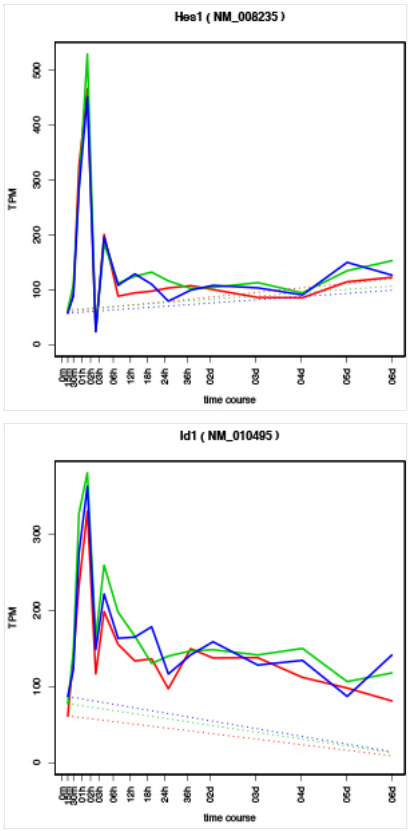

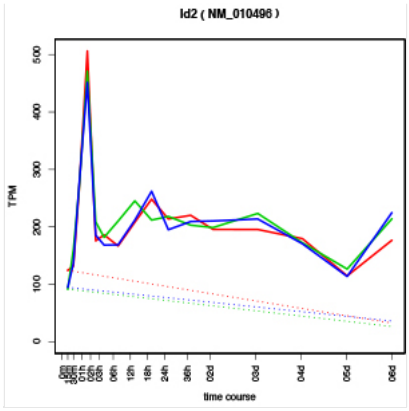
Id2 (NM_010496)
TPM
time course


rep1
rep2
rep3
rep1,
no induction
rep2,
no induction
rep3,
no induction

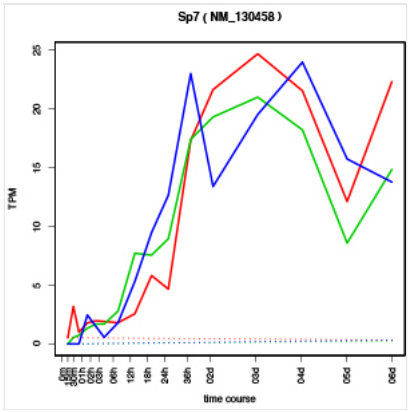
Sp7 (NM_130458)
TPM
time course

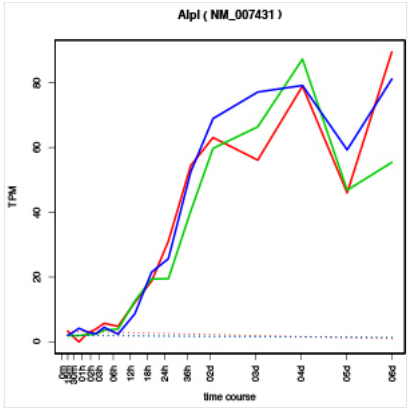
Alpl (NM_007431)
TPM
time course

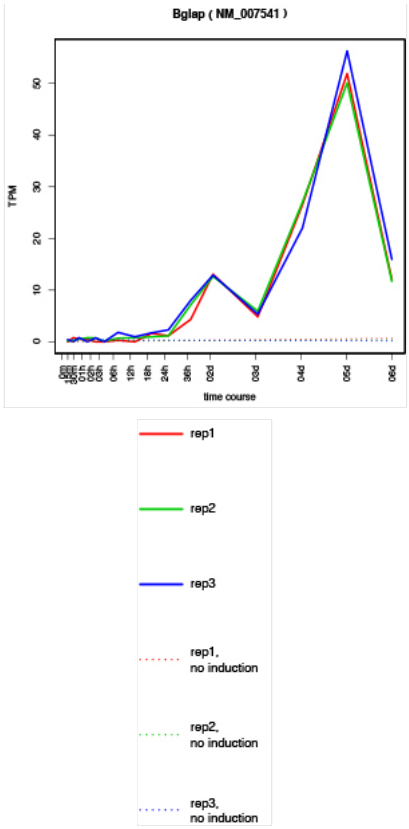

Figurea 4. Gene expression (TPM) of key regulators (*Hes1*, *Id1*, *Id2*,*Sp7*) and differentiation markers (*Alpl*, *Bglap*).

References

1. Burkhardt R, Kettner G, Bohm W, Schmidmeier M, Schlag R, et al. Changes in trabecular bone, hematopoiesis and bone marrow vessels in aplastic anemia, primary osteoporosis, and old age: a comparative histomorphometric study. Bone (1987) 8(3):157-164. PMID:3606907

2. Nuttall ME, Gimble JM. Controlling the balance between osteoblastogenesis and adipogenesis and the consequent therapeutic implications. Curr Opin Pharmacol (2004) 4(3):290–294. PMID:15140422

3. Tokuzawa Y, Yagi K, Yamashita Y, Nakachi Y, Nikaido I, et al. Id4, a new candidate gene for senile osteoporosis, acts as a molecular switch promoting osteoblast differentiation. PLoS Genet (2010) 6(7):e1001019. PMID:20628571

4. Mizuno Y, Yagi K, Tokuzawa Y, Kanesaki-Yatsuka Y, Suda T, et al. miR-125b inhibits osteoblastic differentiation by down-regulation of cell proliferation. Biochem Biophys Res Commun (2008) 368(2):267-272. PMID:18230348.

Ciliated epithelium timecourse

Differentiation of basal cells to tracheal ciliated cells

Time course ID: mouse_Tracheal_epithelial_cells
Sample provider: Mitsuru Morimoto

Introduction

The vertebrate cilium is a sensory and mechanical organelle critical for a broad array of homeostatic mechanisms. Although such a biological importance of ciliogenesis is well investigated, molecular processes of ciliogenesis has been remained in mystery. Notch signaling plays a crucial role in alternative ciliated or secretory cell fate determination from bi-potential progenitor in developing lung epithelium. Using mouse tracheal epithelial primary culture cells (mTECs) that allow us to examine airway mucociliary epithelial cell differentiation from its progenitor cells in in vitro, we successfully established high-efficient ciliated cell induction culture system with pharmacological inhibition of Notch signaling. Taking advantage of this culture system, we harvested time-course samples from differentiating ciliated cells at 18 time points after the differentiation induction and harvested total RNA from these.

Samples

The detailed protocol for the mTECs culture has been published by Vladar and Brody, 2013. mTECs are isolated from the tracheas removed from female mice between 12~20 weeks of age. mTECs were cultured on 12-well plates, 1.00 x 105 /well, containing Transwell permeable membrane supports (Corning). Within 5 days, the cells become confluent and differentiation was induced by removing serum and growth factors from the medium. For hyper induction of ciliated cells, 10 uM of gamma secretase “DAPT” was added into the medium. At the time points after differentiation induction, total RNA was extracted by lysing mTECs with QIAzol Lysis Reagent and purified by the miRNeasy kit (QIAGEN).

Quality control

Known marker genes: FoxJ1 [2] and Mcidas [3].

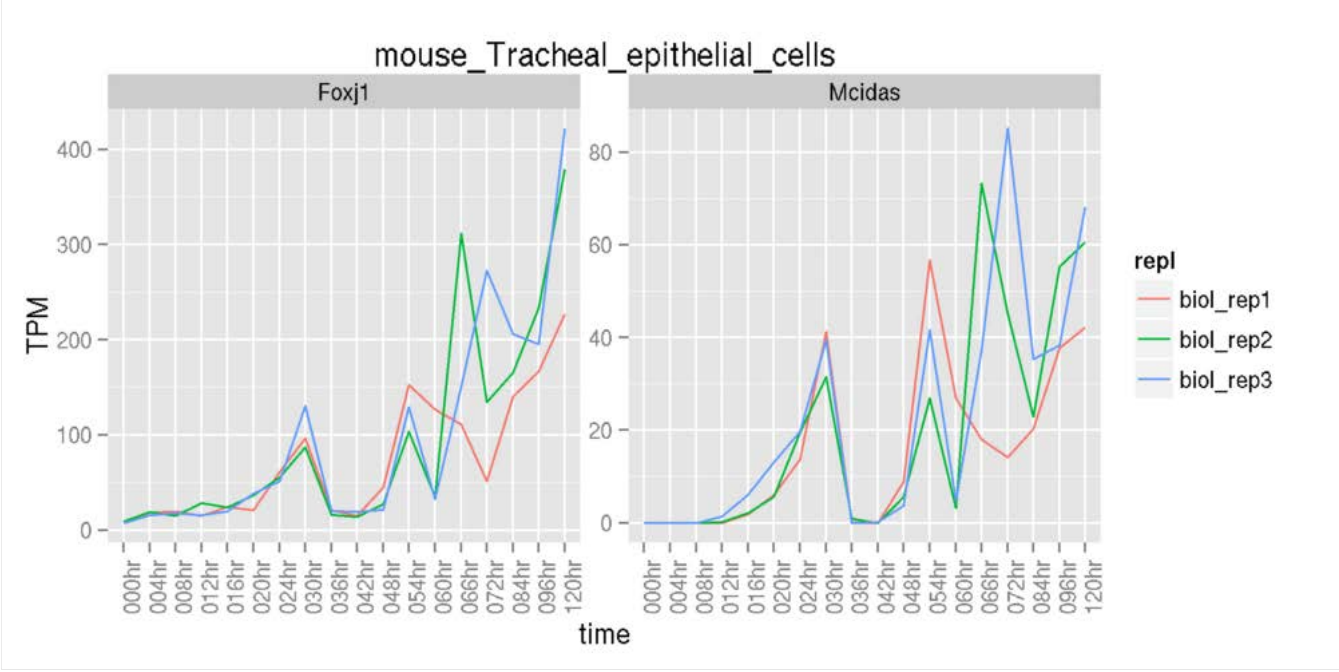

Figure 1: CAGE expression of marker genes in TPM.

References

[1] Vladar EK and Brody SL, Analysis of ciliogenesis in primary culture mouse tracheal epithelial cells. Methods Enzymol. 2013;525:285-309.

[2] You Y, Huang T, Richer EJ, Schmidt JE, Zabner J, Borok Z, Brody SL. Role of f-box factor foxj1 in differentiation of ciliated airway epithelial cells. Am J Physiol Lung Cell Mol Physiol. 2004 Apr;286(4):L650-7. Epub 2003 Jun 20.

[3] Stubbs JL, Vladar EK, Axelrod JD, Kintner C. Multicilin promotes centriole assembly and ciliogenesis during multiciliate cell

differentiation. Nat Cell Biol. 2012 Jan 8;14(2):140-7. doi: 10.1038/ncb2406.

Trophoblast timecourse

Time course ID: mouse_trophoblast_stem_cell_line
Sample provider: Mitsuhiro Endoh, Tamie Endoh, Haruhiro Koseki

Introduction

During mouse development, the implanting blastocyst embryo is composed of the inner cell mass (ICM) and the outer trophectoderm (TE) layer. Permanent stem cell lines can be derived from these two lineages; embryonic stem (ES) cells from ICM [1] [2] and trophoblast stem (TS) cells from TE [3]. TS cells can differentiate into multiple cell types only of the trophoblast lineage, while ES cells can differentiated into all three germ layer cell types. TS cells grow in the presence of fibroblast growth factor (FGF) 4 and mouse embryonic fibroblast-conditioned medium (MEF-CM). Removal of FGF4 and MEF-CM from the TS cell culture medium causes them to differentiate in vitro into trophoblast giant cells and other trophoblast subtypes. We want to investigate how gene expression is controlled in the trophoblast lineage. To do this we conducted a timecourse analysis of gene expression profiles of TS cells after the removal of FGF4 and MEF-CM.

Samples

TS cell lines are maintained in an undifferentiated state in the presence of FGF4 and 70% MEF-CM, and are differentiated by removal of FGF4 and MEF-CM for 0, 1, 2, 3, 4, 5, or 6 days (total 7 points). We used following three TS cell lines: a wild-type female TS cell line “B1”, a wild-type male TS cell line “Rybp”, and an Ring1A-/- male TS cell line “R1AB” (Ring1A-/- mice are healthy and exhibit no apparent phenotype in placental tissues [4]) .

Quality control

List of published key marker genes for your time course, if available with references:

- Cdx2, Eomes, Esrrb, Fgfr2: Marker genes for undifferentiated TS cells [3]
- Prl3d1, Prl3b1, Prl2c2: Marker genes for trophoblast giant cells [5] [6]
- Tpbpa: The Tpbpa gene is expressed in ectoplacental cone cells starting between embryonic days (E) 7.5 and 8.5, and later in the spongiotrophoblast layer of the mature placenta [7]
- Ascl2: The Ascl2 gene is expressed in the ectoplacental cone, the chorion and their derivatives in the placenta [8]

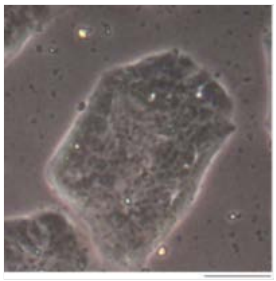

Figure 1: B1 TS cells day0 (undifferentiated; scale bar = 100 um)

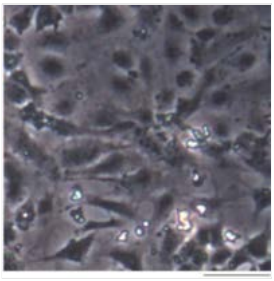

Figure 2: B1 TS cells day5-differentiation (scale bar = 100 um)

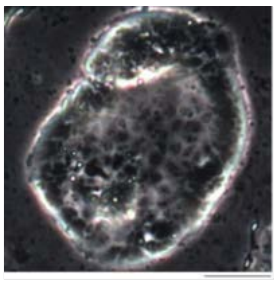

Figure 3: R1AB TS cells day0 (undifferentiated; scale bar = 100 um)

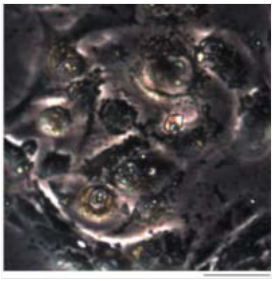

Figure 4: R1AB TS cells day5-differentiation (scale bar = 100 um)

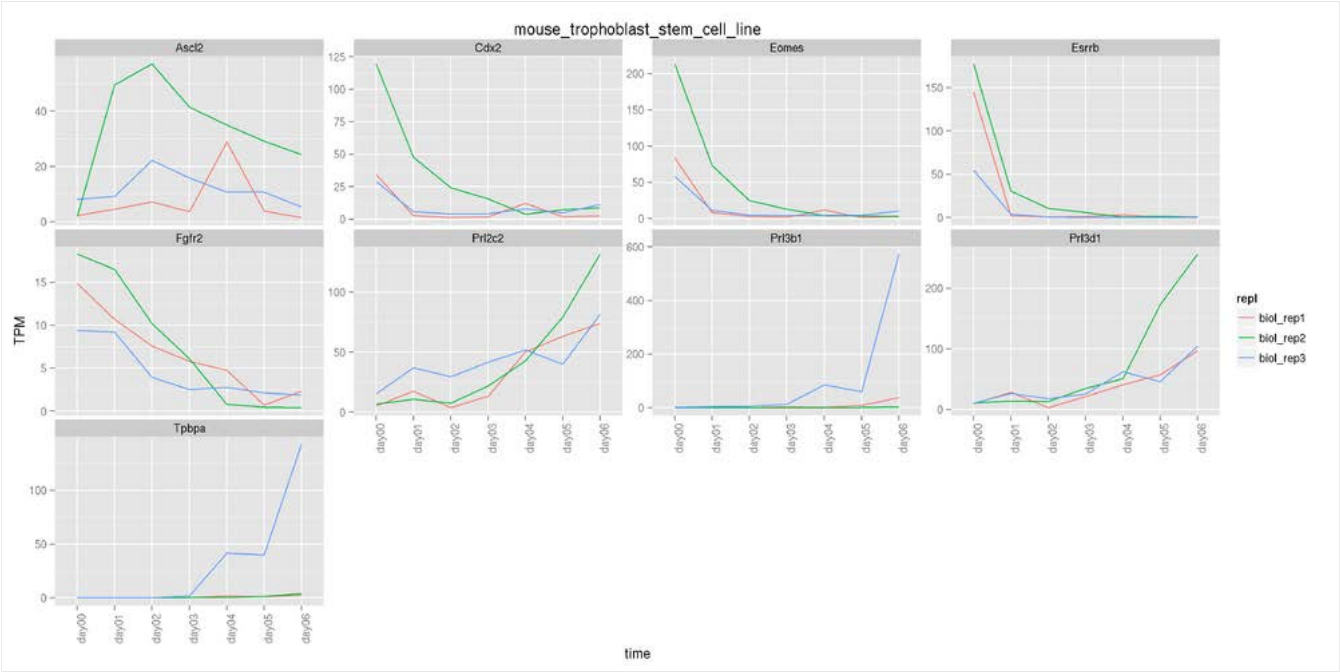

Figure 5: CAGE expression of marker genes in TPM.

References

[1] Evans MJ and Kaufman MH. Establishment in culture of pluripotential cells from mouse embryos. Nature. 1981. 292(5819): p154-6.

[2] Martin GR. Martin, Proc Natl Acad Sci U S A. 1981. 78(12): p7634-8.

[3] Tanaka S. Promotion of trophoblast stem cell proliferation by FGF4. Science. 1998. 282(5396): p2072-5.

[4] del Mar Lorente M, Marcos-Gutiérrez C, Pérez C, Schoorlemmer J, Ramírez A, Magin T, Vidal M. Loss- and gain-of-function mutations show a polycomb group function for Ring1A in mice. Development. 2000. 127(23): p5093-100.

[5] Faria TN, Ogren L, Talamantes F, Linzer DI, Soares MJ. Localization of placental lactogen-I in trophoblast giant cells of the mouse placenta. Biol Reprod. 1991. 44(2), p327-31

[6] Hu D and Cross JC. Development and function of trophoblast giant cells in the rodent placenta. Int J Dev Biol. 2010. 54(2-3): p341-54

[7] Hu D and Cross JC. Ablation of Tpbpa-positive trophoblast precursors leads to defects in maternal spiral artery remodeling in the

mouse placenta. Dev Biol. 2011. 358(1): p231-9

[8] Guillemot F, Nagy A, Auerbach A, Rossant J, Joyner AL. Essential role of Mash-2 in extraembryonic development. Nature 1994. 371 (6495): p.333-6

Visual cortex development

Time course ID: mouse_visual_cortex
Sample provider: Alka Saxena, Michela Fagiolini

Introduction

Objective

The main objective of this project was to identify differentially expressed genes in the visual cortex of the Mecp2 knockout (KO) mouse at three developmental ages (Postnatal day 14 (P14), P30 and P60) critical for the maturation and regression of visual system and to characterize any variations in TSS usage in the Mecp2 KO mouse during development using the newly developed Helicos-CAGE technology [1].

Background

Mutations in the Methyl CpG binding protein 2 (MECP2) gene cause Rett Syndrome, a severe neuro-developmental disorder caused by impaired synaptic plasticity [2]. MeCP2, a member of the Methyl CpG binding domain family of proteins, is able to bind methylated and non-methylated DNA [3-6]. The MeCP2-DNA interaction results in chromatin compaction, which is correlated with silencing of chromatin. Binding of MeCP2 to chromatin also stabilizes the chromatin structure and protects from nuclease digestion [3].

The role of MeCP2 in transcription regulation has been studied extensively. ChIP-Chip studies done on differentiated SHSY5Y cells on customized microarrays reveal that MeCP2 binds mainly to inter-genic regions and that most promoters associated with MeCP2 are transcriptionally active [7]. Studies done on the expression profile of Mecp2 null, Mecp2 transgenic (tg) and wild type animals reveal that 85% of the total genes mis-regulated in mecp2 mouse models show a profile consistent with an unexpected transcriptional activator-like role for Mecp2 [8]. These data obtained from mouse hypothalamus, were confirmed by extensive quantitative PCR analysis and Mecp2 binding was confirmed with ChIP-qPCR. Bisulfite sequencing analysis showed that active MeCP2 target promoters were not methylated [8]. However, recent ChIP-seq studies conducted in brain revealed that Mecp2 binds all over the genome in a uniform manner but shows specific enrichment peaks in methylated regions [9, 10] while ChIP-seq in astrocytes reveals that MeCP2 binds to specific gene targets [11] thus suggesting a cell specific role for MeCP2. Altogether there is uncertainty about the role of MeCP2 in transcriptional regulation and binding to specific targets. MeCP2 appears to bind transcriptionally active as well as inactive regions of the genome; but whether it participates in the regulation of expression of specific target genes needs more investigation. If MeCP2 regulates the transcription of key genes involved in synaptic plasticity, it is important to identify them for the design of therapeutic targeting strategies and to gain insights into the molecular pathogenesis of Rett Syndrome and other disorders associated with MECP2 mutations. Our project aimed to address this uncertainty by using state of the art sequencers and newly developed “omics” technology.

The mouse visual cortex provides an extraordinary opportunity in this research. Plasticity in the visual cortex can be manipulated by dark /light rearing of mice and studied using standard electrophysiological techniques and this tissue holds immense promise as a system for manipulation and monitoring of plasticity through therapeutic drugs and targeted gene therapy. Physiological and behavioral studies conducted by Dr. Michela Fagiolini on the visual cortex of mecp2 null male mice reveal an "apparent" normal development of visual cortical plasticity from P14 until P30 when vision rapidly begins to regress together with the onset of the general Rett syndrome phenotype. By P60 Mecp2 KO mice exhibit a full regression [12]. These three ages also correspond to three phases of visual cortex development and plasticity: pre-critical period, critical period and adulthood. Thus the visual cortex represents a characterized region of the brain in terms of plasticity impairment related to Mecp2 deficiency and we aimed to conduct our studies in the visual cortex of male wild type and mecp2 null mice. In this project we analyzed the transcriptome at the three critical stages of visual cortex development: P14, P30 and P60; which is expected to provide us with a comprehensive picture of the transcriptional irregularities that commence before and after the onset of electrophysiological changes.

Significance

Our studies have the potential to identify genes mis-regulated before the onset of behavioral changes, track changes in gene expression as development proceeds and also identify any variations in transcriptional start site usage before and after the onset of symptoms in the mouse visual cortex. At its conclusion, it will provide a comprehensive understanding of the molecular pathways leading to impairment in developmental plasticity in the visual cortex of mecp2 null mice. We expect to identify a few key genes / pathways involved in synaptic plasticity and regulated by mecp2 which will provide future directions towards targeted therapy for this disorder.

Samples

RNA was extracted from the visual cortex dissected from wildtype and Mecp2 KO mice (B6;129P2-Mecp2tm1Bird/J) at the ages P14, P30

and P60. Dissected tissue was flash frozen in liquid nitrogen and shipped on Dry ice. RNA was extracted using Trizol and Qiagen RNAeasy columns with some modifications designed to retain small RNAs. Table 1 depicts the numbers of samples used.

Sample type	wild type	MeCP2 knockout (bird Model)
Visual cortex P14	4	3
Visual cortex P30	3	3
Visual cortex P60	3	3
Total samples	10	9

Table-1: Number of samples in each subgroup in the visual cortex time course

Quality control

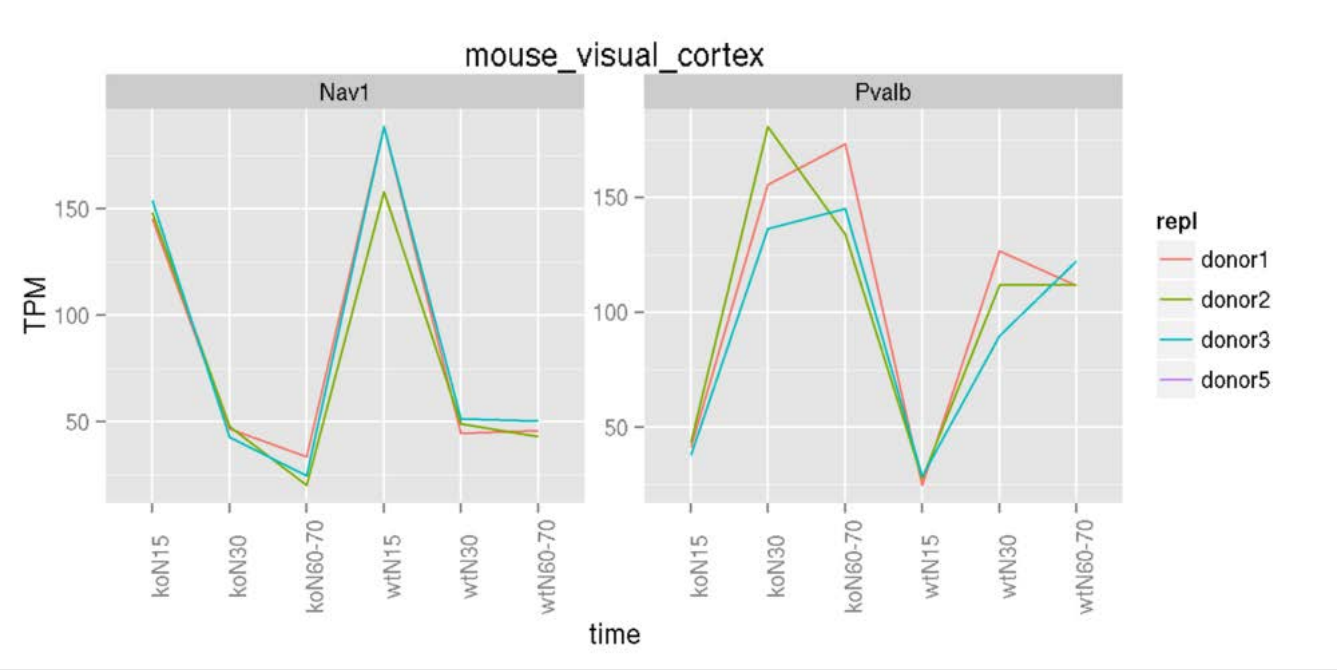

Figure 1: CAGE expression of marker genes in TPM.

- Pvalb - ref up regulated (parvalbumin neuron-specific marker)
- Nav1 - down regulated (Mouse neuron navigator 1, a novel microtubule-associated protein involved in neuronal migration. "expression is largely restricted to the NS during development." PMID: 15797708)

References

[1] Kanamori-Katayama M, Itoh M, Kawaji H, Lassmann T, Katayama S, Kojima M, Bertin N, Kaiho A, Ninomiya N, Daub CO et al: Unamplified cap analysis of gene expression on a single-molecule sequencer. Genome Res 2011, 21(7):1150-1159.

[2] Amir RE, Van den Veyver IB, Wan M, Tran CQ, Francke U, Zoghbi HY: Rett syndrome is caused by mutations in X-linked MECP2, encoding methyl-CpG-binding protein 2. Nat Genet 1999, 23(2):185-188.

[3] Georgel PT, Horowitz-Scherer RA, Adkins N, Woodcock CL, Wade PA, Hansen JC: Chromatin compaction by human MeCP2. Assembly of novel secondary chromatin structures in the absence of DNA methylation. J Biol Chem 2003, 278(34):32181-32188.

[4] Jones PL, Veenstra GJ, Wade PA, Vermaak D, Kass SU, Landsberger N, Strouboulis J, Wolffe AP: Methylated DNA and MeCP2 recruit histone deacetylase to repress transcription. Nat Genet 1998, 19(2):187-191.

[5] Nan X, Tate P, Li E, Bird A: DNA methylation specifies chromosomal localization of MeCP2. Mol Cell Biol 1996, 16(1):414-421.

[6] Nikitina T, Shi X, Ghosh RP, Horowitz-Scherer RA, Hansen JC, Woodcock CL: Multiple modes of interaction between the methylated DNA binding protein MeCP2 and chromatin. Mol Cell Biol 2007, 27(3):864-877.

[7] Yasui DH, Peddada S, Bieda MC, Vallero RO, Hogart A, Nagarajan RP, Thatcher KN, Farnham PJ, Lasalle JM: Integrated epigenomic analyses of neuronal MeCP2 reveal a role for long-range interaction with active genes. Proc Natl Acad Sci U S A 2007, 104(49):19416-19421.

[8] Chahrour M, Jung SY, Shaw C, Zhou X, Wong ST, Qin J, Zoghbi HY: MeCP2, a key contributor to neurological disease, activates and

represses transcription. Science 2008, 320(5880):1224-1229.

[9] Cohen S, Gabel HW, Hemberg M, Hutchinson AN, Sadacca LA, Ebert DH, Harmin DA, Greenberg RS, Verdine VK, Zhou Z et al: Genome-wide activity-dependent MeCP2 phosphorylation regulates nervous system development and function. Neuron 2011, 72(1):72-85.

[10] Skene PJ, Illingworth RS, Webb S, Kerr AR, James KD, Turner DJ, Andrews R, Bird AP: Neuronal MeCP2 is expressed at near histone-octamer levels and globally alters the chromatin state. Mol Cell 2010, 37(4):457-468.

[11] Yasui DH, Xu H, Dunaway KW, Lasalle JM, Jin LW, Maezawa I: MeCP2 modulates gene expression pathways in astrocytes. Mol Autism 2013, 4(1):3.

[12] Durand S, Patrizi A, Quast KB, Hachigian L, Pavlyuk R, Saxena A, Carninci P, Hensch TK, Fagiolini M: NMDA Receptor Regulation Prevents Regression of Visual Cortical Function in the Absence of Mecp2. Neuron 2012, 76(6):1078-1090.